

12.13 Biomarker-Based Inferences of Past Climate: The Alkenone $p\text{CO}_2$ Proxy

M Pagani, Yale University, New Haven, CT, USA

© 2014 Elsevier Ltd. All rights reserved.

12.13.1	Introduction	361
12.13.2	The Alkenone CO_2 Proxy	361
12.13.2.1	Roots of the Methodology	361
12.13.2.2	Models of Algal Carbon Isotope Fractionation Assuming Diffusive Carbon Transport	362
12.13.2.3	Development of the Alkenone- CO_2 Proxy	364
12.13.2.4	The Calibration of 'b' and Estimates of ϵ_f	365
12.13.3	CO_2 Reconstructions, Uncertainties, and Complications	366
12.13.3.1	The Influence of Growth Rate and Irradiance	368
12.13.3.1.1	Dilute cultures and mesocosm experiments	368
12.13.3.1.2	Ocean and surface sediment data	369
12.13.3.1.3	The case against growth rate as the dominant influence on $\epsilon_{p37:2}$	369
12.13.3.2	Consideration of Cell Geometry Changes on Long-Term $\epsilon_{p37:2}$ Records	370
12.13.4	Active Transport and the Case Against the Diffusive Model of Carbon Uptake	372
12.13.4.1	Models for Active Carbon Uptake	373
12.13.5	Summary	374
References		375

12.13.1 Introduction

Descriptive climate reconstructions of ancient Earth do more than evoke steamy images of geothermal pools and dense tropical forests – they serve to tune our perspectives on the climate system itself and what we can expect from our future. Paleoclimatologists are perpetually looking for ways to quantitatively constrain these images and consider how the edges of climate and life have moved from where we are today. How we quantify depends on our discipline, but some of our best methodologies derive from geochemistry and the influence that environmental conditions exert on the rate and equilibria of chemical reactions. Advocates of geochemical proxies strive to establish precise tools with clean edges that leave no ambiguity, and interpretations are often presented as such. But geochemical signals are rarely unidimensional and biological interactions are always close at hand. For the advancement of new geochemical proxies, it is often convenient to ignore biological interactions because the inevitable influence of organisms is vexing. For some, however, the messiness of life is something to embrace.

Organic geochemists have made it their business to reveal environmental signals buried in the distribution of organic compounds and their chemistries, and it is now apparent that some organic debris has much to say about the environmental conditions in which it formed or decayed, with surprising accuracy. Organic proxies used to determine ancient environmental conditions, such as sea-surface temperatures or carbon dioxide concentration, require a full accounting of associated uncertainties including the range of other physical and chemical parameters impacting the proxy, a detailed accounting of the organisms that produce the organic signal, as well as extensive tests of the proxy across the environmental and temporal bounds that constrain their habitat and evolution. These are large tasks and never fully accomplished, but periodic updates

on our accumulated knowledge help determine where we need to go next. In that spirit, this chapter focuses on the stable carbon isotopic composition of alkenones designed to constrain ancient atmospheric carbon dioxide concentrations. These proxies, and others designed to detect similar signals, are becoming increasingly important as we strive to understand Earth's climate sensitivity to CO_2 forcing and how it has changed through time.

12.13.2 The Alkenone CO_2 Proxy

12.13.2.1 Roots of the Methodology

Early efforts to explain the stable carbon isotopic character of marine plankton in terms of temperature (Sackett, 1986; Sackett et al., 1965) led to an appreciation of the roles that dissolved CO_2 concentration (Calder and Parker, 1973; Degens et al., 1968a,b; Deuser et al., 1968; Pardue et al., 1976; Rau et al., 1982), growth rate (Pardue et al., 1976; Wong and Sackett, 1978), and metabolic pathways (Falkowski, 1991; Wong and Sackett, 1978) play in determining the magnitude of carbon isotopic fractionation during photosynthesis. Arthur et al. (1985) and Dean et al. (1986) were the first to apply these early findings, using $\delta^{13}\text{C}$ values of kerogen to argue for distinctly higher CO_2 concentrations during the Cretaceous – an interpretation consistent with the emerging realization of the time that greenhouse gas forcing likely drove the notable warmth of greenhouse climates (Barron and Washington, 1985; Berner, 1991; see Chapter 6.13). Their interpretation of higher CO_2 was founded on isotopic analyses indicating that Cretaceous sediments dominated by well-preserved marine organic carbon were more ^{13}C -depleted than modern or Cretaceous-age terrestrial organic carbon. Similar isotopic relationships were also noted for other warm periods such as the Devonian (Maynard, 1981). These observations of Cretaceous

organic carbon isotopes represented a reversal in relative isotopic relationships between terrestrial and marine organic carbon observed today, where terrestrial carbon is typically more ¹³C-depleted than marine carbon – a pattern arguably established by the Miocene (Arthur et al., 1985; Dean et al., 1986). Continued application of bulk organic carbon (C_{org}) δ¹³C values as a proxy for surface water CO₂ generated closer inspection of the controls on plankton δ¹³C values, requiring complementary efforts by geologists, geochemists, and plant/algal physiologists.

Measurements in natural settings that showed an inverse relationship between ¹³C/¹²C composition of freshwater plankton with the logarithmic concentration of surface water aqueous CO₂ ([CO_{2aq}]) (McCabe, 1985), and an inverse, but linear relationship between marine algae δ¹³C and [CO_{2aq}] in open marine environments (Rau et al., 1989), set the stage for more quantitative inferences of ancient CO₂ based on sedimentary organic carbon (Rau et al., 1991). Bulk sedimentary δ¹³C records were shown to approximate interglacial/glacial CO₂ variability (Rau et al., 1991), demonstrating the validity of this approach. However, bulk sedimentary organic matter is a compromised medium given that it is a diagenetic composite of carbon (e.g., Emerson et al., 1987) from multiple organisms – marine, bacterial, and terrestrial. Arthur et al. (1985) and Dean et al. (1986) spent considerable effort assessing the degree of diagenetic alteration and the influence of terrestrial carbon before settling on their interpretations specific to Cretaceous CO₂, and all subsequent bulk analyses required similar considerations (Rau et al., 1991; Raymo et al., 1996). These realities and the difficulties of diagenesis were present in the minds of organic geochemists, and a more accurate partitioning of sedimentary organic carbon was increasingly desired.

The new discipline of compound-specific isotope analyses emerged contemporarily with bulk organic studies (e.g., Des Marais et al., 1980; Freeman et al., 1990; Hayes et al., 1987; Matthews and Hayes, 1978; Popp et al., 1989). Specific compounds exhibited a broad range of isotopic compositions due to differences in provenance and compound classes (Freeman et al., 1990), and further cautioned against CO₂ estimates based on bulk organic carbon. In contrast, compound-specific records held the promise of a diagenetically free isotopic signal from highly specific sources.

The first long-term, compound-specific isotope record focused on carbon isotope signatures of geoporphyryns (diagenetic derivatives of chlorophyll) from the Cretaceous Western Interior seaway (Hayes et al., 1989). This work, in conjunction with a theoretical model of algal isotope fractionation, was then used to interpret CO₂ history (Hayes et al., 1989; Popp et al., 1989).

12.13.2.2 Models of Algal Carbon Isotope Fractionation Assuming Diffusive Carbon Transport

Total carbon isotope fractionation between the carbon substrate (dissolved inorganic carbon, DIC) and organic carbon associated with carbon fixation can be approximated by the term Δ_{DIC-org} where

$$\Delta_{\text{DIC-org}} = \delta^{13}\text{C}_{\text{DIC}} - \delta^{13}\text{C}_{\text{org}} \quad [1]$$

or explicitly defined as the variable ε_p in relation to aqueous carbon dioxide (Freeman and Hayes, 1992; Popp et al., 1989):

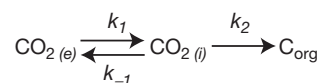
$$\varepsilon_p = \left(\frac{\delta^{13}\text{C}_{\text{CO}_{2\text{aq}}} + 1000}{\delta^{13}\text{C}_{\text{org}} + 1000} \right) \times 1000 \quad [2]$$

δ¹³C_{org} can be directly measured in geologic archives, but δ¹³C_{CO_{2aq}} cannot and requires a proxy such as the δ¹³C value of coeval carbonate minerals with an assumption of equilibrium during the transformation of DIC or aqueous carbon dioxide to solid carbonate.

The first low-resolution, long-term reconstruction of ε_p from geoporphyryns from various marine sediments (Popp et al., 1989) yielded temporal patterns that confirmed earlier isotopic observations (Arthur et al., 1985) and ultimately mirror alkenone-based (Pagani et al., 2005) and bulk organic (Hayes et al., 1999) studies performed a decade later (Figure 1).

Compound-specific ε_p values are not directly comparable with bulk sedimentary ε_p values because lipids are ¹³C-depleted relative to bulk photosynthate (DeNiro and Epstein, 1977; Park and Epstein, 1961). However, once isotopic corrections are applied to bulk data (see Hayes et al., 2001), broad trends and absolute values are in general agreement (Figure 1) even though bulk signals are subject to diagenetic processes (Hayes, 1993; Hayes et al., 1999). The broad correspondence among the available ε_p records is remarkable (Figure 1) and likely reflects forcing at the global scale given that the data derive from a range of algal communities from different regions of the world.

Interpretations of algal ε_p values are founded on a model that describes the total carbon isotope fractionation that occurs during C₃ photosynthesis in higher plants (Farquhar et al., 1982, 1989). This perspective describes fractionation in terms of the flow or flux of carbon, including the movement of carbon into the cell and back out to the environment (i.e., leakage), and the flow of inorganic carbon that is ultimately fixed as organic carbon. Figuratively, carbon fluxes can be described as:



where CO_{2(e)} represents the ambient CO_{2aq} concentration (often represented as C_e), CO_{2(i)} is the concentration of CO_{2aq} inside the cell (often represented as C_i), k₁, k₋₁ are the rate constants for the flux of carbon into and out of the cell, and k₂ is the rate constant for the flux of carbon fixed as organic carbon. From this perspective, ε_p can be expressed in terms of the fraction of the intracellular carbon reservoir fixed as organic matter or lost due to back diffusion (leakage), and the isotope fractionations occurring during carbon transport and fixation (Farquhar et al., 1982; Francois et al., 1993) can be expressed as

$$\varepsilon_p = \varepsilon_f + f(\varepsilon_f - \varepsilon_t) \quad [3]$$

where the terms ε_f and ε_t represent the carbon isotope fractionations associated with carbon fixation and diffusive transport, and f is the fraction of intracellular inorganic carbon that diffuses back into the environment. The term f can be described in terms of carbon fluxes:

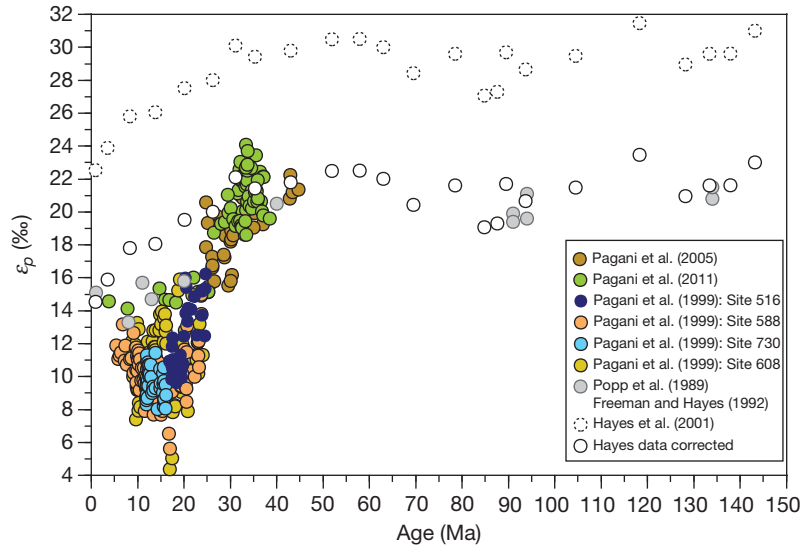


Figure 1 Compilation of long-term ε_p values from alkenones (colored symbols; Pagani et al., 1999, 2005, 2011), geoporphyryns (gray symbols; Popp et al., 1999) and bulk organic carbon (open symbols; Hayes et al., 1999). Hayes et al. corrected data applies an offset of 8‰ to calculate lipid ε_p values.

$$f = \frac{k_{-1}C_i}{k_1C_e} \quad [4]$$

in which case, eqn [3] can also be described in terms of CO_2 concentrations:

$$\varepsilon_p = \varepsilon_t + (\varepsilon_f - \varepsilon_t) \frac{C_i}{C_e} \quad [5]$$

where k_1 is assumed to equal k_{-1} , and C_i and C_e are the intracellular and environmental concentrations of CO_{2aq} .

The goal, in the context of algal CO_2 proxies, is to determine C_e from ε_p . However, the path to interpretation requires a detailed consideration of C_i . Assuming that intracellular concentration of CO_{2aq} arrives by simple diffusion, C_i derives from a diffusion flux (J) of carbon:

$$J = -D \frac{\partial C}{\partial x} \quad [6]$$

where ∂C is the inorganic carbon gradient across the cell membrane (i.e., $C_e - C_i$), and D is the diffusion coefficient. The diffusion flux into a volume requires consideration of surface area, which for unicellular photosynthetic organisms is a function of cell geometry. C_i is also modulated by specific growth rate, which consequently ranks as a critical lever on the value of ε_p . In addition, other isotopic complications can arise if limiting levels of C_i trigger other physiological responses (e.g., active carbon transport) that enhance carbon availability in addition to the diffusion flux of CO_{2aq} . Indeed, active transport, or the capacity to actively increase the concentration of C_i (discussed below), is characteristic of the majority of algae studied and complicates assumptions of diffusive carbon flux. However, even if a predominant diffusion model is assumed, it is clear that the extracellular concentration of CO_{2aq} is not the sole determinant of C_i for unicellular organisms.

Efforts to model the impact of carbon demand have explored the physiological variables that influence C_i and the diffusion flux of carbon. Rau et al. (1992) defined carbon demand in terms of $(C_e - C_i)$ and considered the impact of

carboxylation rate (i.e., growth rate) by redefining the term C_i/C_e by its algebraic equivalent:

$$\varepsilon_p = \varepsilon_t + (\varepsilon_f - \varepsilon_t) \left(1 - \frac{C_e - C_i}{C_e}\right) \quad [7]$$

Francois et al. (1993) further defined the rate of carboxylation (G) as:

$$G = k_1C_e - k_{-1}C_i \quad [8]$$

where k represents the resistance to diffusion across the cell membrane, which is assumed to be the same entering or leaving the cell ($k_{-1} = k_1$), and relates to the permeability of the cell membrane.

Laws et al. (1995, 1997) expanded on earlier work and expressed specific growth rate (μ) in terms of the flux of CO_{2aq} relative to the carbon content:

$$\mu = \frac{k_1C_e - k_{-1}C_i}{C} \quad [9]$$

where C is the carbon content of the cell. If, as assumed by Francois et al. (1993), k_1 and k_{-1} are equivalent for diffusion flux, then eqn [7] becomes:

$$\varepsilon_p = \varepsilon_t + (\varepsilon_f - \varepsilon_t) \left(1 - \frac{\mu C}{kC_e}\right) \quad [10]$$

Here, diffusion flux of CO_{2aq} is assumed proportional to the permeability of the cell membrane (P), which is arguably related to cellular surface area (S) (Laws et al., 1995, 1997), while the carbon content of the cell (C) is proportional to the cellular volume (V) (Verity et al., 1993; Popp et al., 1998a). Therefore, eqn [10] can be recast as:

$$\varepsilon_p = \varepsilon_t + (\varepsilon_f - \varepsilon_t) \left(1 - \frac{\mu C}{PC_e}\right) \quad [11]$$

or

$$\varepsilon_p = \varepsilon_t + (\varepsilon_f - \varepsilon_t) \left(1 - \frac{\mu V}{C_e S}\right) \quad [12]$$

The impact of surface area on the carbon isotopic composition of algae was first explored by Riebesell et al. (1993) and then included in an integrated model by Rau et al. (1996) which further explored the role of cell volume and membrane permeability, among other variables. Ultimately, these models demonstrate the potential impact that non-CO₂ variables play in the expression of ε_p and subsequent calculations of ancient carbon dioxide concentrations.

Equation [5] and subsequent transformations assume diffusive carbon transport to the site of carboxylation. But, as stated above, there is a substantial body of work that demonstrates that carbon transport can be physiologically mediated in order to concentrate intracellular CO₂. We address this topic further on, but first consider the assumptions and history that promoted the basis of alkenone-CO₂ proxy.

12.13.2.3 Development of the Alkenone-CO₂ Proxy

Various theoretical models of carbon fixation provide a framework for interpreting ε_p values, but initially, ε_p was empirically correlated to solely ambient CO₂ concentrations. Empirical relationships between ε_p and [CO_{2aq}] (eqn [13]) were based on results from lacustrine settings (Hollander and McKenzie, 1991; McCabe, 1985) and took the logarithmic form:

$$\varepsilon_p = A[\log(\text{CO}_{2\text{aq}})] + B \quad [13]$$

Assuming that eqn [13] is generally valid, variables A and B can be estimated for a particular marine setting (e.g., Freeman and Hayes, 1992; Jasper and Hayes, 1990) and interpretations of ancient CO₂ levels can be made from both bulk- (Raymo et al., 1996) and biomarker-derived (Freeman and Hayes, 1992) ε_p records. Initial efforts to reconstruct ancient CO₂ also included the application of ε_p values based on the isotopic composition of the alkenone biomarker (Jasper and Hayes, 1990).

The application of alkenones in CO₂ reconstruction was recognized as a significant step forward given early recognition that alkenone production is limited to few algae, thus reducing diverse algal influences on the expression of ε_p . Alkenones are unsaturated ethyl and methyl ketones with 37–39 carbon atoms (C₃₇–C₃₉) primarily synthesized in the ocean's mixed layer by only some species of haptophyte algae (Conte et al., 1994). Today, alkenones are predominantly produced by *Emiliania huxleyi* (from the Late Pleistocene to the present; Thierstein et al., 1977) and *Gephyrocapsa oceanica* (from the Pliocene to the present; Hay, 1977) and are found in measurable abundances in Neogene to mid-Paleogene marine sediments (Pagani et al., 1999, 2005, 2011; Seki et al., 2010). Alkenones found in sediments that predate the origin of modern species were presumably produced by ancient relatives, and examination of sediments extending to the mid-Eocene containing both alkenones and nannofossils narrowed the probable source to the family Noelaerhabdaceae and genera *Reticulofenestra* and *Dictyococcites* (Marlowe et al., 1990; Young, 1990, 1998).

Alkenones are also widely applied as a proxy for mean-annual sea-surface temperature (see Chapter 8.15). The alkenone temperature proxy, U^K₃₇, is based on the ratio of the di- and tri-unsaturated abundances (Prahl and Wakeham, 1987). The unsaturation state of lipids impacts its melting point and it was first proposed that alkenone unsaturation helps to regulate membrane fluidity (Marlowe et al., 1984).

However, alkenones have not been detected in haptophyte membranes. Instead, it has been proposed that these lipids are metabolic storage molecules and that their unsaturation state has functional relationships to melting point and the ease at which the molecules are catabolized (Epstein et al., 2001). It is also known that other nontemperature parameters, such as nutrient stress and light availability, impact the concentrations of alkenones and relative abundances of their unsaturated forms (Prahl et al., 2003).

Alkenones, as well as all lipids, are ¹³C-depleted relative to whole-cell isotope compositions ($\delta^{13}\text{C}_{\text{org}}$; eqn [2]), and thus calculation of ε_p from the carbon isotope composition of alkenones requires knowledge of the isotopic difference between $\delta^{13}\text{C}_{\text{C}_{37:2}}$ and $\delta^{13}\text{C}_{\text{org}}$ ($\Delta\delta$):

$$\delta_{\text{org}} = \left[(\delta_{\text{C}_{37:2}} + 1000) \left(\frac{\Delta\delta}{1000} + 1 \right) \right] - 1000 \quad [14]$$

A $\Delta\delta$ value of 4.2‰ for diunsaturated alkenones (C_{37:2}) is commonly applied in paleo-CO₂ reconstructions (Bijl et al., 2010; Pagani et al., 2005, 2009, 2011; Seki et al., 2010) following the work of Jasper and Hayes (1990), Jasper et al. (1994), Bidigare et al. (1997), and Popp et al. (1998b). Popp et al. (1998b) found no growth rate effects on $\Delta\delta$; however, other values for $\Delta\delta$ have been measured in cultures and range from 3.1‰ to 5.9‰ (Riebesell et al., 2000; Schouten et al., 1998; Van Dongen et al., 2002) and one mesocosm bloom experiment showed $\Delta\delta$ (between C_{37:2} and particulate organic carbon) increasing from 7‰ to 12‰ during stationary growth (Benthien et al., 2007). Variability in the value of $\Delta\delta$ of this magnitude can have considerable impact on CO₂ calculations, particularly if ε_p is high (e.g., approaching values of maximum carbon isotope fractionation). Whether or not significant variability of $\Delta\delta$ is expressed in natural systems or over geologic time is unknown.

The first application of C_{37:2} as a CO₂ proxy attempted to assess confidence in the methodology by reconstructing Holocene and Pleistocene CO₂ glacial/interglacial patterns (Jasper and Hayes, 1990). Alkenone-based ε_p records ($\varepsilon_{p\text{C}_{37:2}}$) were reconstructed from $\delta^{13}\text{C}$ values of C_{37:2} and surface-dwelling foraminifera from sediments in the northern Gulf of Mexico. CO₂ estimates were calculated using eqn [13] by determining the value of constants A and B through comparison of CO₂ data from the Vostok ice core. This work was followed by a study of sediments from the central equatorial Pacific Ocean in order to determine patterns of air-sea CO₂ disequilibrium during the Pleistocene and to promote a more simplified theoretical model of carbon isotope fractionation (Jasper et al., 1994). Model simplifications of eqn [5] and similar equations were necessary because carbon demand, C_i , and other physiological factors (eqns [11] and [12]) are unconstrained. Accordingly, Jasper et al. (1994) defined a simplified expression:

$$\varepsilon_p = \varepsilon_f - \frac{b}{C_e} \quad [15]$$

The term ' b ,' equivalent to $(C_e - C_i)(\varepsilon_f - \varepsilon_i)$, integrates all physiological variables affecting the total carbon isotope fractionation during photosynthesis (Bidigare et al., 1997; Jasper et al., 1994). A functional form of eqn [15] was developed by estimating values of ε_f and the physiological-dependent term ' b ' by comparison with published sedimentary alkenone-based

ε_p values (Jasper and Hayes, 1990), water column POC-based ε_p values, and CO_2 data (Rau et al., 1992), and then applied assuming invariable membrane permeability and growth rate. Results from CO_2 records developed by this approach implicated significant variations in equatorial air–sea disequilibrium over glacial/interglacial cycles, but perhaps more important was the convincing success of this more simplified theoretical model. To date, eqn [15] remains the algebraic form for estimating CO_2 from alkenone-based ε_p values.

12.13.2.4 The Calibration of ‘ b ’ and Estimates of ε_f

Marked advances in paleo- CO_2 reconstructions developed from more detailed inspections of the controls on $\delta^{13}\text{C}_{37:2}$ and $\varepsilon_{p37:2}$ with the specific intent to understand the factors driving carbon isotope fractionation in alkenone-producing algae (Bidigare et al., 1997). Chemostat incubations of *E. huxleyi* – the dominant alkenone-producing haptophyte algae in the modern ocean – performed under constant irradiance, assessed the impact of growth rate (threefold variation controlled by steady-state nitrate concentrations) and $[\text{CO}_{2\text{aq}}]$ (28-fold range) on ε_p values (Bidigare et al., 1997). This work and other chemostat experiments provided support for the theoretical relationships expressed by eqn [10] for *E. huxleyi*, and diatoms *Phaeodactylum tricornutum* (Laws et al., 1997) and *Porosira glacialis* (Popp et al., 1998a), and showed that under specific conditions, ε_p can vary linearly with $\mu/\text{CO}_{2\text{aq}}$ (eqn [10]). Results also highlight stark differences in the slope of ε_p versus $\mu/\text{CO}_{2\text{aq}}$ among different algae forced by differences in the proportion of cell volume to surface area (eqn [12]) (Popp et al., 1998a). However, for the eukaryotes studied, ε_f (the maximum fractionation largely attributable to the enzyme Rubisco and other carboxylases) converges on a value of 25‰.

Isotopic responses measured in natural haptophyte populations (Bidigare et al., 1997, 1999) also helped support the simplified model of isotopic fractionation (eqn [15]) by demonstrating linear relationships between the physiological-dependent term ‘ b ’ and the concentration of reactive soluble phosphate ($[\text{PO}_4^{3-}]$; Figure 2). The role of $[\text{PO}_4^{3-}]$, or perhaps

some other covarying biolimiting trace nutrient (Bidigare et al., 1997), implicates growth rate as a key variable influencing $\varepsilon_{p37:2}$ for natural haptophyte populations, consistent with experimental results.

The results of Bidigare et al. (1997) and other efforts (e.g., Eek et al., 1999; Laws et al., 2001; Popp et al., 1999) allow a calibration of the variable ‘ b ’ in terms of $[\text{PO}_4^{3-}]$ (Table 1). The geometric mean regression of ‘ b ’ versus $[\text{PO}_4^{3-}]$, where $b = (\varepsilon_f - \varepsilon_p)C_e$, requires an assumption regarding the value of ε_f , which varies depending on the number and form of enzymes involved. The application of other ε_f values impacts the calculated value of ‘ b ’ and both the slope and intercept of the $b/[\text{PO}_4^{3-}]$ regression (Table 1). Understanding isotope fractionations associated with individual enzymes is key to determining a value for ε_f .

Rubisco (ribulose 1,5-bisphosphate carboxylase/oxygenase), the principal carbon-fixing enzyme, has four phylogenetic forms distributed among Eukarya, Archaea, and Bacteria with Forms I and II directly associated with the Calvin–Benson–Bassham reductive pentose phosphate pathway during autotrophic carbon fixation (Badger and Bek, 2008). Form I, the most abundant variant, is found in Eukarya and Bacteria (Tabita et al., 2008). Form I Rubisco is subdivided into four subforms (IA, B, C, and D), with subform ID associated with ‘nongreen’ algae including coccolithophores, diatoms, rhodophytes, and select dinoflagellates (Boller et al., 2011 and references therein). Multiple forms of Rubisco likely evolved in response to environmental stresses related to changes in atmospheric $[\text{CO}_2]$ and $[\text{O}_2]$ throughout Earth history (Badger and Bek, 2008; Young et al., 2012), and subsequently express a broad range of isotope discrimination related to the form’s

Table 1 ε_f and the geometric mean regression of ‘ b ’ versus $[\text{PO}_4^{3-}]$

ε_f value (‰)	Geometric mean regression
25	$b = (118.52[\text{PO}_4^{3-}]) + 84.07$
27	$b = (129.00[\text{PO}_4^{3-}]) + 105.58$
28	$b = (135.66[\text{PO}_4^{3-}]) + 115.45$

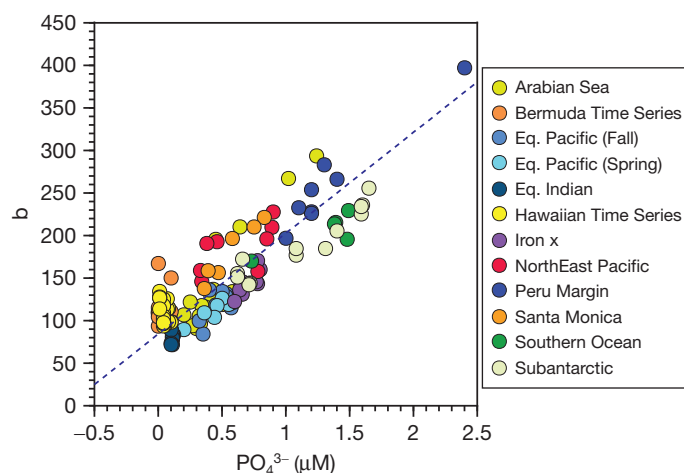


Figure 2 Compilation of ‘ b ’ versus soluble phosphate for natural haptophyte populations calculated using $\varepsilon_f = 25\text{‰}$. Solid line represents the geometric mean regression. If different values of ε_f are assumed, the term ‘ b ’ is recalculated and the equation for the ‘ b ’ versus $[\text{PO}_4^{3-}]$ regression is altered (see Table 1). Data from Bidigare et al. (1997), Popp et al. (1999), Eek et al. (1999), and Laws et al. (2001).

CO_2/O_2 specificity (Boller et al., 2011; Tcherkez et al., 2006). For example, Form IB Rubisco associated with terrestrial plants has a fractionation factor (α) equivalent to 1.029 ($\epsilon = \sim 29\text{‰}$) (Farquhar et al., 1989; Raven and Johnston, 1991; Roeske and O'Leary, 1984), but in total, Forms IA and IB express an ϵ range from 22‰ to 29‰ (Roeske and O'Leary, 1984; Scott et al., 2004, 2007), and Form II shows a 18–22‰ range (Guy et al., 1993; McNevin et al., 2006; Robinson et al., 2003; Roeske and O'Leary, 1984). In contrast, recent analysis of Form ID – the Rubisco associated with *E. huxleyi* and other algae – found a maximum fractionation of $\sim 11\text{‰}$ (Boller et al., 2011). This surprisingly small ^{13}C discrimination conflicts with long standing perspectives and data that argue for much higher enzymatic fractionations during algal growth. For example, Goericke et al. (1994) calculated an ϵ_f range of 25–28‰ for algae with C_3 -type metabolisms, considering a 2–10% contribution of β -carboxylation to the total carboxylation (e.g., Tsuji et al., 2009). However, if an $\sim 11\text{‰}$ enzymatic fractionation for haptophytes is valid, then processes that remove ^{13}C from the cell would be necessary to achieve the ϵ_p values (from 7‰ to 25‰) determined in controlled cultures (Bidigare et al., 1997; Hinga et al., 1994; Riebesell et al., 2000; Rost et al., 2002) and paleo-reconstructions (Pagani et al., 1999, 2005, 2011). Boller et al. (2011) suggest that more ^{13}C -depleted signatures could be accomplished, in part, by the excessive production and excretion of ^{13}C -enriched polysaccharides involved in the production of coccoliths, which is favored under nitrogen limitation (see Benthien et al., 2007) and potentially high irradiance. Still, this mechanism is estimated to raise $\delta^{13}\text{C}$ values by only $\sim 4\text{‰}$ (Boller et al., 2011) and cannot account for higher observed ϵ_p values in the ancient record (Figure 1) or naked haptophyte strains (Bidigare et al., 1997). Clearly, additional experimentation is necessary to determine if the controversial result of Boller et al. (2011) is valid.

12.13.3 CO_2 Reconstructions, Uncertainties, and Complications

If the results of Boller et al. (2011) prove to be robust and characteristic of natural haptophyte populations, then it implies that cellular carbon budgets and CO_2 concentration cannot necessarily explain the magnitude and variability of ϵ_p expressed in the geologic record (Figure 1). This challenges the application of alkenone-derived CO_2 reconstructions unless the process of ^{13}C -enrichment is somehow linked to CO_2 concentration. However, there remains a long history of algal culture experiments that support CO_2 variability as a principal lever on the expression of ϵ_p (e.g., Degens et al., 1968a,b; Hinga et al., 1994; Pardue et al., 1976; Popp et al., 1998a; Riebesell et al., 2000). Chemostat experiments (Bidigare et al., 1997; Laws et al., 1997; Popp et al., 1998a) show clear linear relationships between ϵ_p and $\mu/\text{CO}_{2\text{aq}}$ modulated by cell geometry (Popp et al., 1998a), consistent with theory, and converge on an ϵ_f value of $\sim 25\text{‰}$ as growth rate approaches zero. On the basis of these results and previous experimental data and considerations (Goericke et al., 1994), alkenone-based paleo- CO_2 reconstructions have assumed ϵ_f values in the range of 25–28‰ (Pagani et al., 1999, 2011; Seki et al., 2010; Figure 3).

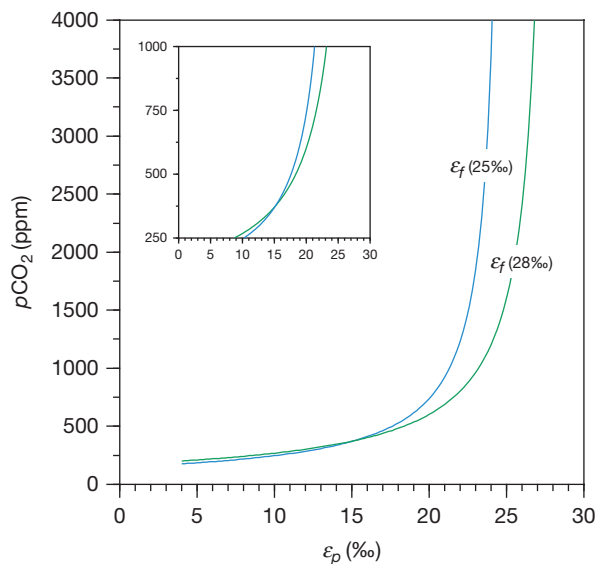


Figure 3 Effect of ϵ_f values on alkenone-based CO_2 estimates. Calculations use expressions of 'b' listed in Table 1 and assume $[\text{PO}_4^{3-}] = 0.3$ and temperature = 20°C . Inset shows an expanded view of the y-axis.

Alkenone- CO_2 reconstructions based on eqn [15] assume that (1) the diffusive model of carbon isotope fractionation is appropriate for alkenone-producing algae across time and place, (2) the global 'b' versus $[\text{PO}_4^{3-}]$ relationship (Figure 2) represents a mean approximation of regional conditions over time, and (3) the range of values for ϵ_f (i.e., 25–28‰) that define the calibration of 'b' are reasonably constrained. Conversion of ancient $\epsilon_{p37:2}$ values to $[\text{CO}_{2\text{aq}}]$ and $p\text{CO}_2$ requires estimates of surface water phosphate concentrations and temperature. In general, ancient $[\text{PO}_4^{3-}]$ are assumed to be the same as the modern range within the photic zone for a particular ocean locality (Pagani et al., 1999; Seki et al., 2010). These estimates can be further refined by considering differences in paleoceanographic conditions, biogeochemical ocean modeling (Pagani et al., 2011), Sr/Ca variations (Stoll and Schrag 2000), and, in one case, dinocyst assemblages (Bijl et al., 2010).

Temperature estimates, necessary to calculate $\delta^{13}\text{C}_{\text{CO}_{2\text{aq}}}$ from $\delta^{13}\text{C}_{\text{CaCO}_3}$ and $p\text{CO}_2$ from $[\text{CO}_{2\text{aq}}]$ (e.g., Pagani et al., 1999), rely on other proxies such as carbonate $\delta^{18}\text{O}$ values, TEX_{86} or U_{37}^k , and come with potentially significant uncertainties. If ϵ_p values are low, uncertainties in SST result in relatively small uncertainties in $p\text{CO}_2$ reconstructions, but as $\epsilon_{p37:2}$ values approach the assumed value for ϵ_f , uncertainties in sea-surface temperature and $[\text{PO}_4^{3-}]$ become increasingly relevant (Figure 4).

Consideration of the sum of uncertainties associated with the methodology suggests a range of CO_2 uncertainty between 20% and 30% for ϵ_p values below 20‰ when CO_2 levels are relatively low and phosphate concentrations are reasonably constrained (Freeman and Pagani, 2005). Uncertainty significantly increases as the value of ϵ_p approaches the assumed value of ϵ_f , reflecting the decrease in sensitivity at high ϵ_p values (Figures 3 and 4).

Efforts to assess the accuracy of the alkenone- CO_2 proxy by reconstructing Pleistocene to Holocene CO_2 have returned positive, but mixed results. Pleistocene $\epsilon_{p37:2}$ data from the

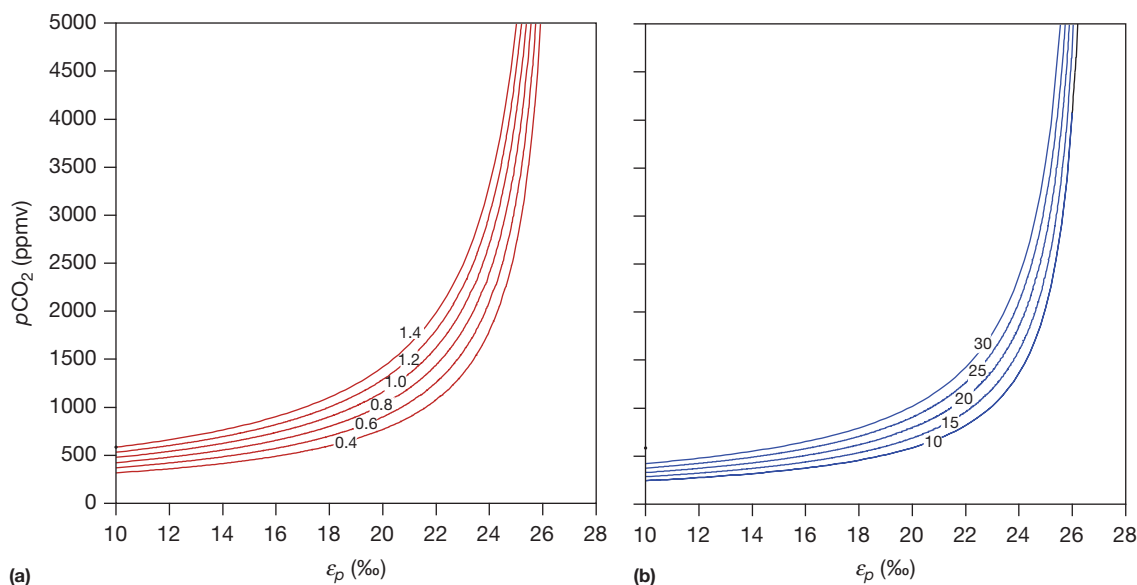


Figure 4 Relationships between ϵ_p , temperature, and phosphate. Figures assume $\epsilon_f = 25\%$. (a) Relationship between ϵ_p and $p\text{CO}_2$ for a range of phosphate (0.4–1.4 $\mu\text{mol kg}^{-1}$). (b) Relationship between ϵ_p and $p\text{CO}_2$ for a range of temperature (10–30 $^{\circ}\text{C}$).

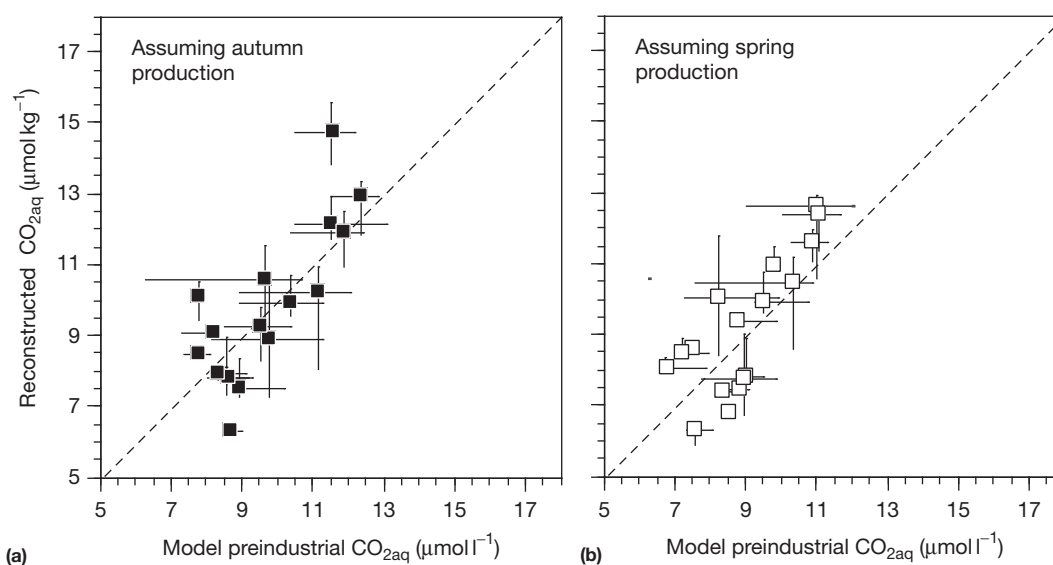


Figure 5 Cross-plot of modeled preindustrial $[\text{CO}_{2\text{aq}}]$ versus alkenone-based $[\text{CO}_{2\text{aq}}]$ using an $\epsilon_f = 25\%$, respectively. (a) Autumn production assumed. (b) Spring production assumed. Dashed line represents a 1:1 correlation. Modified from Pagani M, Freeman KH, Ohkouchi K, and Caldeira K (2002) Comparison of water column $[\text{CO}_{2\text{aq}}]$ with sedimentary alkenone-based estimates: A test of the alkenone- CO_2 proxy. *Paleoceanography* 17: 1069. <http://dx.doi.org/10.1029/2002PA000756>.

equatorial Pacific Ocean (Jasper et al., 1994, discussed above) were later reconsidered by Stoll and Schrag (2000), who corrected for growth rate changes through Sr/Ca analysis of planktonic foraminifera. Reconstructed CO_2 was shown to track ice core data, but explained only 30–35% of the variance reflected in the Vostok record for the past 250 000 years (Laws et al., 2002; Stoll and Schrag, 2000). In contrast, Pagani et al. (2002) evaluated the capacity of alkenone data to mimic preindustrial water column $[\text{CO}_{2\text{aq}}]$ patterns using surface sediments across a central North Pacific Ocean meridional transect and found that the proxy was generally accurate. Depth of alkenone

production, determined from temperature-depth profiles and U_{37}^k temperatures, was used to identify phosphate concentrations as well as $\delta^{13}\text{C}$ of $\text{CO}_{2\text{aq}}$. Alkenone-reconstructed $[\text{CO}_{2\text{aq}}]$ was lower than modern values, but within 20% of modeled preindustrial water column values (Figure 5).

If the diffusive model of carbon fractionation is assumed valid, offsets between observed and reconstructed records could reflect the importance of other environmental factors that impact ϵ_p , including growth rate, irradiance, and cell size. These other factors can potentially dominate ϵ_p variability, especially if $[\text{CO}_{2\text{aq}}]$ is low with relatively small variability.

Alternatively, offsets between observed and calculated CO_2 could also imply that a model of diffusive carbon uptake is not entirely correct (discussed below).

12.13.3.1 The Influence of Growth Rate and Irradiance

12.13.3.1.1 Dilute cultures and mesocosm experiments

While results of chemostat cultures support a diffusion model for some algae under certain conditions, other experiments and field data have been less supportive. Dilute batch cultures return significantly different results. Burkhardt et al. (1999a) cultured marine diatoms *A. glacialis*, *T. punctigera*, *C. waiilesii*, *P. tricorutum*, and the dinoflagellate *S. trochoidea* under variable irradiance and nutrient-replete conditions with the intent to separate the individual influences of CO_2 and growth rate. Results demonstrated that $[\text{CO}_{2\text{aq}}]$ was still a leading variable influencing ϵ_p values. However, growth rate and cell size had an equivalent or greater impact on isotopic fractionation relative to CO_2 concentration. Irradiance cycle and daylight length, presumably impacting growth rate, was also shown to be as important as $[\text{CO}_{2\text{aq}}]$ (Burkhardt et al., 1999b). Similar to chemostat incubations, dilute cultures of *E. huxleyi* show that ϵ_p is inversely impacted by $\text{CO}_{2\text{aq}}$ and $\mu/\text{CO}_{2\text{aq}}$ (Riebesell et al., 2000), but the ϵ_p versus $\mu/\text{CO}_{2\text{aq}}$ relationship was nonlinear with substantially lower ϵ_p values and ϵ_f estimates (estimated as μ/CO_2 approaches zero) compared to results from nutrient-limited, chemostat incubations (Figure 6). In addition, light intensity and light cycle, independent of growth rate, was shown to have a more significant impact on ϵ_p values for *E. huxleyi* than either CO_2 variability or growth rate, with CO_2 showing negligible influence even though $[\text{CO}_2]$ varied from 5 to $34 \mu\text{mol l}^{-1}$ (Rost et al., 2002). Interestingly, ϵ_p increased with increasing μ and μ/CO_2 , in opposition to the diffusion theory of fractionation (Figure 7). A similar positive correlation between ϵ_p and μ/CO_2 was reported for dilute batch cultures of *G. oceanica* (also an alkenone-producing coccolithophore; Figure 8), while results for *Coccolithus pelagicus* ssp. *braarudii* were more consistent with predictions of eqn [10] (Rickaby et al., 2010).

Mesocosm bloom experiments dominated by populations of *E. huxleyi* were conducted under a range of CO_2 conditions

from 180 to 710 ppmv (Benthien et al., 2007) and $\epsilon_{p37.2}$ systematically decreased during the exponential growth phase following patterns of nutrient utilization and presumably increased growth rate. In this work, $\epsilon_{p37.2}$ values were offset (albeit by only 2‰ by the end of the exponential growth phase) between CO_2 experiments, but both CO_2 and nutrient concentrations decreased during blooms resulting in only an ~ 200 ppm difference between end member experiments by the end of the exponential growth period. Higher $\epsilon_{p37.2}$ values were associated with higher CO_2 content, confirming expectations of the influence of CO_2 . However, a much larger $\epsilon_{p37.2}$ response was associated with nutrient utilization compared to CO_2 (Benthien et al., 2007).

Dilute cultures and mesocosm experiments highlight the importance of growth and physiological effects on the magnitude of ϵ_p and cast further suspicion on the theoretical basis of the $\epsilon_{p37.2}$ -based CO_2 reconstructions. However, results of chemostat incubations are supportive (i.e., Popp et al., 1998a) and

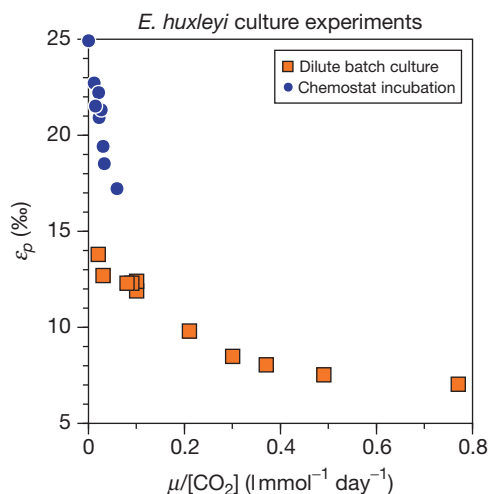


Figure 6 Comparison of ϵ_p versus $\mu/[\text{CO}_{2\text{aq}}]$ from chemostat and dilute batch cultures of *E. huxleyi*. Chemostat incubation: circles (Bidigare et al., 1997), conducted under nitrate-limited, continuous light conditions. Dilute batch cultures: squares (Riebesell et al., 2000), performed under nitrate-saturated, 16:8 h light:dark regime.

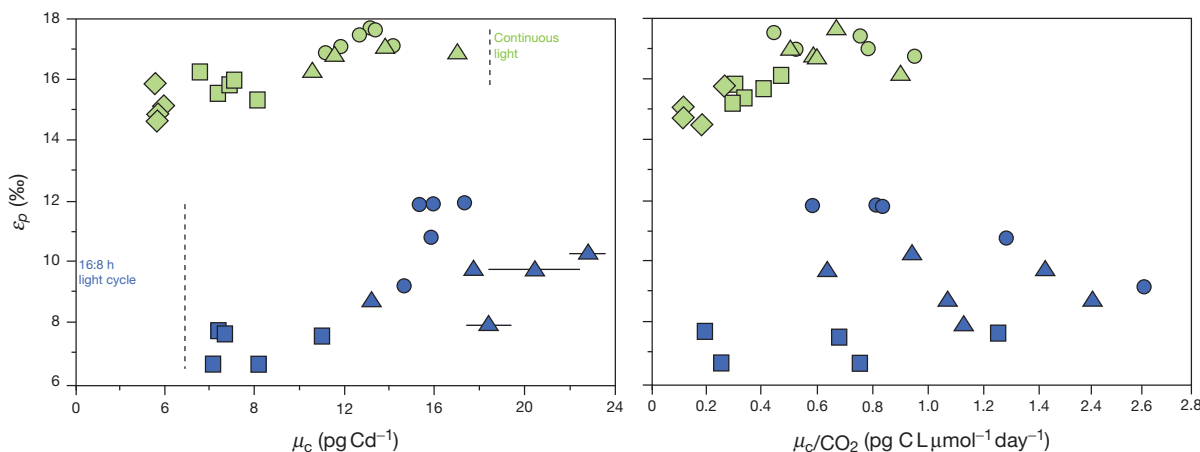


Figure 7 Irradiance experiments on *E. huxleyi*. Modified from Rost et al. (2002).

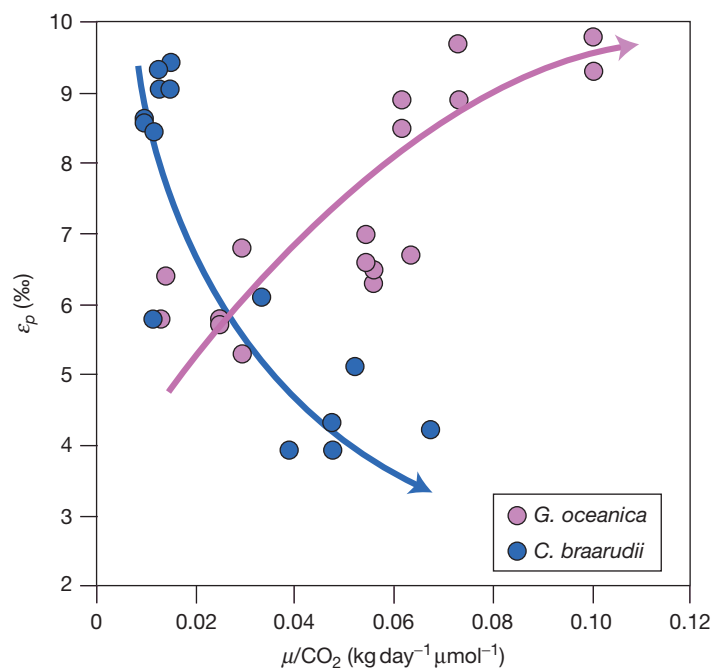


Figure 8 Isotope relationships for coccolithophores *G. oceanica* and *C. braarudii*. Modified from Rickaby et al. (2010).

the sum of experiments indicates that different conditions of growth can trigger different physiological responses to growth rate, nutrient supply, light, and CO_2 . There is no consensus on which experimental design – if any – best mimics natural conditions.

12.13.3.1.2 Ocean and surface sediment data

The accumulation of sea-surface analyses (Bidigare et al., 1997; Laws et al., 2001) provides evidence for an important role for $[\text{PO}_4^{3-}]$ on the isotopic composition of haptophytes, and supports a primary influence for algal growth rate on the expression of ϵ_p . However, field studies indicate that $\epsilon_{p37:2}$ is not strongly correlated with $1/[\text{CO}_{2\text{aq}}]$ (Figure 9(a)) as anticipated by diffusion models (Bidigare et al., 1997; Laws et al., 2001). The available data show a weak correlation of $\epsilon_{p37:2}$ versus $[\text{PO}_4^{3-}]/[\text{CO}_{2\text{aq}}]$ (Figure 9(c)), suggesting either that the dependency of 'b' on $[\text{PO}_4^{3-}]$ is actually driven by an association of $[\text{CO}_{2\text{aq}}]$ with $[\text{PO}_4^{3-}]$ in surface waters (Figure 9(d)), making $[\text{CO}_{2\text{aq}}]$ the primary determinant, or that the ratio $\mu/[\text{CO}_{2\text{aq}}]$ is the ultimate variable as predicted by diffusion models. If the latter is valid, other variables that impact growth rate are likely at play given the rather poor fit between $\epsilon_{p37:2}$ and $[\text{PO}_4^{3-}]/[\text{CO}_{2\text{aq}}]$. For example, Eek et al. (1999) noted that ϵ_p is significantly correlated to $[\text{PO}_4^{3-}]/[\text{CO}_{2\text{aq}}]$ when the concentration of the total concentration of nitrate and nitrite ($[\text{N}]$) is greater than zero, and further implied that metabolic adjustments as nitrogen-bearing, biolimiting nutrients become severely limiting.

Results from surface sediment analyses support the importance of nutrients in determining the value of $\epsilon_{p37:2}$ (Figure 10). $\epsilon_{p37:2}$ values reconstructed from surface sediments from the equatorial and South Atlantic Ocean (Benthien et al., 2002) and central Pacific (Pagani et al., 2002) are negatively correlated with surface water $[\text{PO}_4^{3-}]$, but positively correlated

with $1/[\text{CO}_{2\text{aq}}]$ (Schulte et al., 2004). Again, the $\epsilon_{p37:2}$ versus $1/[\text{CO}_{2\text{aq}}]$ relationship is contrary to expectations assuming a diffusive-uptake model. On this basis, Schulte et al., 2004 argue that $\epsilon_{p37:2}$ values are a better proxy for $[\text{PO}_4^{3-}]$ rather than for carbon dioxide. Clearly, growth rate effects dominate the modern sedimentary and water column signal, but a compilation of long-term $\epsilon_{p37:2}$ records argues against growth rate or the evolution surface water $[\text{PO}_4^{3-}]$ as the primary variable driving changes in magnitude of $\epsilon_{p37:2}$.

12.13.3.1.3 The case against growth rate as the dominant influence on $\epsilon_{p37:2}$

Ancient $\epsilon_{p37:2}$ values exhibit a much broader range than those measured in the modern ocean (Figure 11). Existing records for the modern ocean indicate that $\epsilon_{p37:2}$ values range from 6.5‰ (i.e., eutrophic environments) to 17.8‰ (i.e., oligotrophic environments). $[\text{PO}_4^{3-}]$ and $[\text{CO}_{2\text{aq}}]$ span from 0 to $2.4 \mu\text{mol kg}^{-1}$, and 9.6 to $28.7 \mu\text{mol}$, respectively. Thus, ancient $\epsilon_{p37:2}$ values that fall within the modern $\epsilon_{p37:2}$ range likely reflect similar environmental conditions found in the modern ocean, assuming that the upper and lower bounds of modern $\epsilon_{p37:2}$ values are an expression of physiological effects constrained by the modern range of $[\text{CO}_{2\text{aq}}]$. However, paleo- $\epsilon_{p37:2}$ values lower or higher than the modern range cannot be reasonably explained by growth effects and more likely reflect the influence of carbon dioxide concentrations that deviate from modern conditions. - Pagani et al. (1999) restricted alkenone analysis for the Miocene (~5–23 Ma) to oligotrophic settings in an effort to minimize variability in growth and further restrict the lower bounds of the $\epsilon_{p37:2}$ range (Figure 11). $\epsilon_{p37:2}$ values for the Miocene fall within and below the modern oligotrophic range of 10.8–17.8 (where $[\text{PO}_4^{3-}] \leq 0.2 \mu\text{mol kg}^{-1}$) and suggest that CO_2 conditions were similar to, or lower than, today (assuming no other

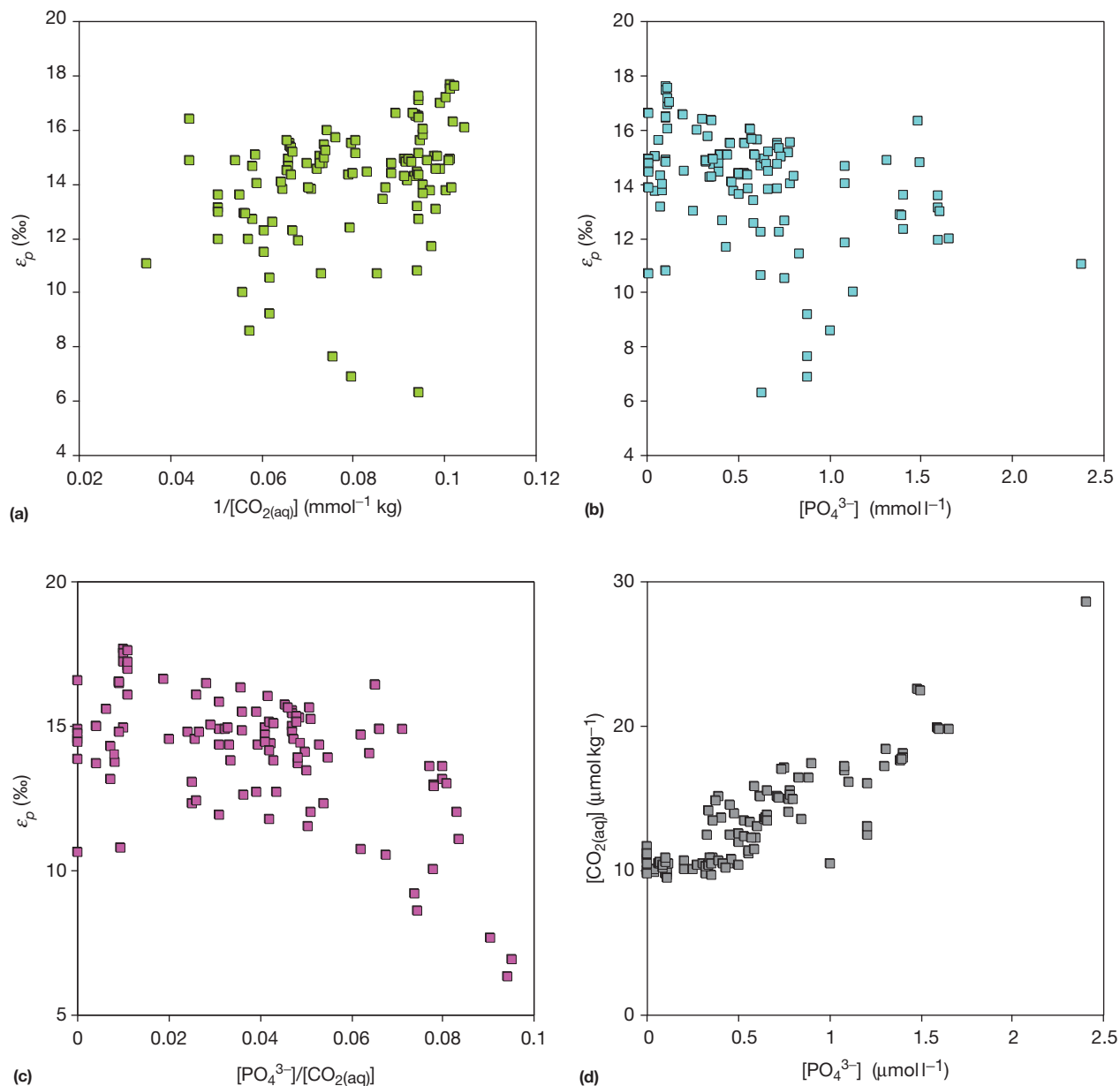


Figure 9 Surface water data associated with $\epsilon_{p37:2}$ values. (a) ϵ_p versus $1/[\text{CO}_2(\text{aq})]$. (b) ϵ_p versus $1/[\text{PO}_4^{3-}]$. (c) ϵ_p versus $[\text{PO}_4^{3-}]/[\text{CO}_2(\text{aq})]$. (d) $[\text{CO}_2(\text{aq})]$ versus $[\text{PO}_4^{3-}]$.

confounding effects). In contrast, $\epsilon_{p37:2}$ values older than ~ 33 Ma derive from both oligotrophic and eutrophic settings. Values higher than the modern range imply even lower growth rates in ancient eutrophic environments relative to those that characterize modern oligotrophic settings, which is unlikely. Viewed from this perspective, whole-ocean changes in nutrients or algal growth rates cannot explain long-term $\epsilon_{p37:2}$ trends, and support an interpretation of higher-than-modern CO_2 concentrations prior to ~ 25 Ma, and similar-to-lower CO_2 conditions for the past 25 My, consistent with interpretations from the earliest publications related to the methodology (Arthur et al., 1985).

12.13.3.2 Consideration of Cell Geometry Changes on Long-Term $\epsilon_{p37:2}$ Records

Given the strong dependency of cell geometry on ϵ_p on both theoretical grounds (eqn [12]) and in culture experiments (Popp et al., 1998a), the possibility that long-term CO_2 interpretations are confounded by the evolution of haptophyte cell size was explored in several publications (Henderiks and Pagani, 2007, 2008; Pagani et al., 2011). Larger cells have a higher volume-to-surface area ratio and should drive ϵ_p values lower (Popp et al., 1998a; eqns [11] and [12]). For example, the long-term decrease in the magnitude of $\epsilon_{p37:2}$

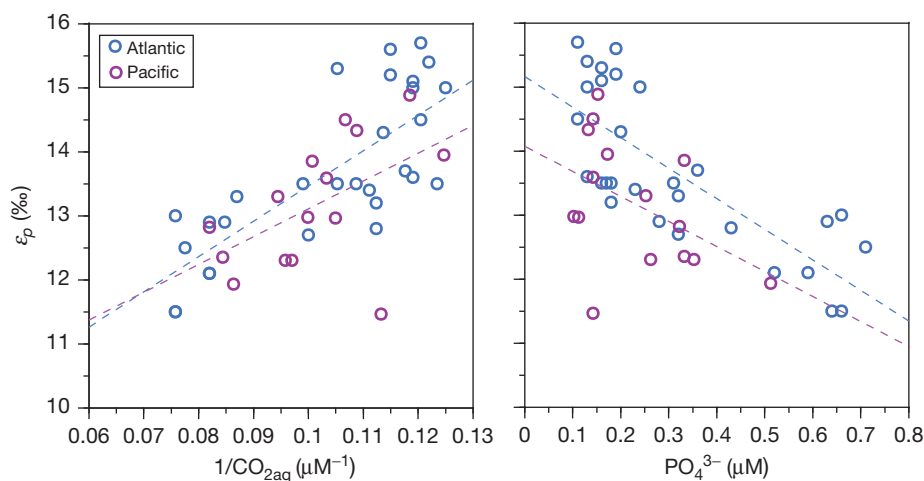


Figure 10 Relationships between sedimentary $\epsilon_{p37:2}$ values, water column $[\text{CO}_{2\text{aq}}]$ and $[\text{PO}_4^{3-}]$. From Shulte et al. (2004). Equatorial Atlantic Ocean data from Benthien et al. (2002); central Pacific Ocean data from Pagani et al. (2002).

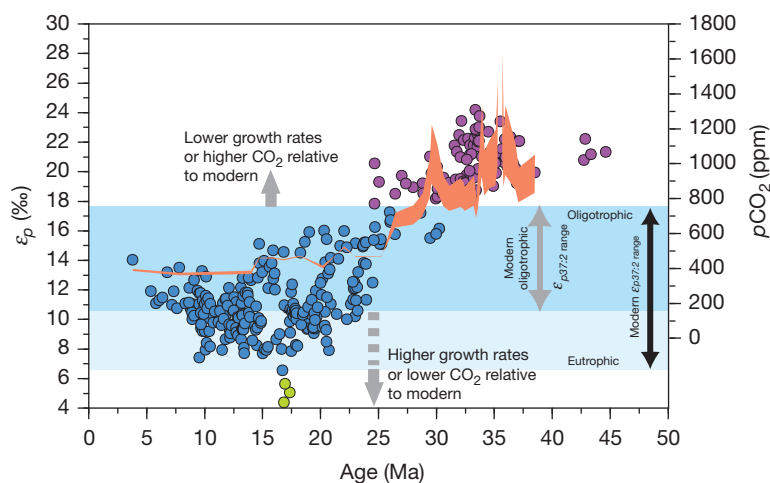


Figure 11 Sedimentary $\epsilon_{p37:2}$ values (filled circles) and $p\text{CO}_2$ calculations for data from Site 925 in the western equatorial Atlantic Ocean (orange band). Different color symbols highlight that ancient data is outside the range of modern $\epsilon_{p37:2}$ values represented by the blue bands. The dark blue band represents the modern range of $\epsilon_{p37:2}$ values from oligotrophic environments where $[\text{PO}_4^{3-}] \leq 0.2 \mu\text{mol kg}^{-1}$. $\epsilon_{p37:2}$ data from Pagani et al. (1999, 2005, 2011).

(Figures 1 and 11) could be explained, in part, by temporally increasing cell diameters of alkenone-producing algae and thus, the ratio of cell volume to surface area. One approach to determining cell size changes utilizes coccolith dimensions in relationship to cell diameter (Henderiks and Pagani, 2007). For alkenone-producing coccolithophores belonging to the Noelaerhabdaceae family, maximum diameter of coccoliths was shown to be a robust proxy of cell size in both modern and ancient species (Henderiks and Pagani, 2007, 2008). Temporal trends for cell sizes using species-specific coccoliths were determined for key sites associated with $\epsilon_{p37:2}$ reconstructions spanning the Middle Eocene to Early Miocene (Henderiks and Pagani, 2007, 2008) and for six sites across the Eocene–Oligocene climate transition (i.e., the climate shift from an ice-free to a fully glaciated Antarctic continent). These efforts demonstrated that changes in cell size cannot explain the observed long-term trends in Paleogene $\epsilon_{p37:2}$. Reticulofenestrids

were shown to display high diversity and the largest mean cell sizes during the Late Eocene with extinctions of very large forms and a long-term decrease in maximum cell size beginning in the latest Eocene/Oligocene (Henderiks and Pagani, 2008; Pagani et al., 2011) – precisely opposite of what would be expected if cell geometry was a primary influence on $\epsilon_{p37:2}$. In fact, if cell geometry played any role in determining the character of $\epsilon_{p37:2}$ values, it did so by minimizing the magnitude of change reflected in $\epsilon_{p37:2}$ trends (Figure 11).

Henderiks and Pagani (2008) suggested that the evolution of smaller algal cells reflected a response to declining CO_2 levels and carbon limitation because smaller diameters increase cellular surface area relative to cell volume. This would be particularly advantageous for algae that largely depend on a diffusive supply of $\text{CO}_{2\text{aq}}$. A similar interpretation was invoked for regional differences in cell sizes for the Eocene–Oligocene climate transition between Antarctic/Subantarctic sites (characterized by

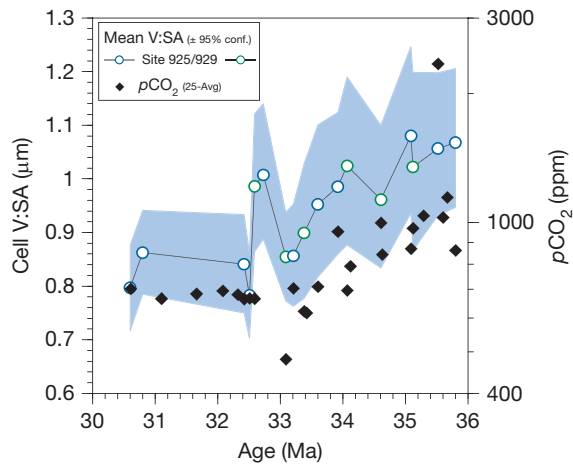


Figure 12 Cell size variability of ancient alkenone-producing algae and estimated $p\text{CO}_2$ levels (using $\epsilon_f = 25\%$) derived from the equatorial Atlantic Sites 925 and 929. Mean cell volume-to-surface area ratios (V:SA, in μm) calculated from mean coccolith length. Shaded blue interval encompasses propagated upper- and lower 95% confidence estimates. Reproduced from Pagani M, Huber M, Liu Z, et al. (2011) The role of carbon dioxide during the onset of Antarctic glaciation. *Science* 334: 1261–1264.

relatively higher $\epsilon_{p37.2}$ values) and the equatorial Atlantic (with relatively lower $\epsilon_{p37.2}$ values). Clear latitudinal differences in mean size and overall size distribution were measured, with the smallest cell diameters found in the equatorial Atlantic (Pagani et al., 2011). Decreasing trends in mean coccolith diameter across the Eocene–Oligocene transition is observed at each site, but is most pronounced in the equatorial Atlantic and appears to resemble the decline in reconstructed CO_2 (Figure 12). Regional offsets in $\epsilon_{p37.2}$ were explained by higher $[\text{CO}_{2\text{aq}}]$ in Antarctic/Subantarctic waters. Alternatively, if similar $[\text{CO}_{2\text{aq}}]$ and ϵ_f values are assumed for both regions, average growth rates would need to have been 40–80% lower in the high southern ocean to explain $\epsilon_{p37.2}$ offsets (Pagani et al., 2011).

If cell size plays an important role in determining the value of $\epsilon_{p37.2}$ as predicted by eqn [12], then the shift during the Eocene to Early Oligocene transition represents a minimum change in $\epsilon_{p37.2}$ and long-term $\epsilon_{p37.2}$ trends are even more difficult to explain by growth rate effects alone.

12.13.4 Active Transport and the Case Against the Diffusive Model of Carbon Uptake

CO_2 reconstructions from $\epsilon_{p37.2}$ records implicitly assume that a diffusion model of carbon uptake is valid for alkenone-producing algae through time (i.e., eqn [11]). However, the concentration of $\text{CO}_{2\text{aq}}$ is the lowest of all dissolved carbon forms available for photosynthesis, constituting $<1\%$ of the total inorganic aqueous pool. For a single cell organism that relies exclusively on diffusion, $\text{CO}_{2\text{aq}}$ supply depends on the diffusion rate through an unstirred boundary layer surrounding the cell (dimensions of which are dependent on the radius of the cell), the production rate of $\text{CO}_{2\text{aq}}$ via HCO_3^-

dehydration both within the cell and the confines of the boundary layer, cell size (i.e., surface area vs. the carbon content), and the permeability of the cell membrane (Wolf-Gladrow and Riesbesell, 1997). Thus, for diffusion transport, the concentration of $\text{CO}_{2\text{aq}}$ at the site of carboxylation is assuredly lower than the ambient concentration outside the cell. This is potentially a problem for sustaining reasonable algal growth rates because the efficiency of carbon fixation by Rubisco is species dependent, but often low. Carbon fixation efficiency is related to the specificity factor of Rubisco – a measure of the selectivity for CO_2 versus O_2 , defined as

$$\tau = \frac{V_{\text{CO}_2} K_{1/2-\text{O}_2}}{V_{\text{O}_2} K_{1/2-\text{CO}_2}} \quad [16]$$

where V is the maximum reaction rates and $K_{1/2}$ is the half-saturation constant (concentration of the substrate where V is half its maximum value). Higher specificity (τ) equates to greater selectivity (affinity) for CO_2 and carbon fixation over photorespiration (Tortell, 2000). Algal Rubisco is known to have a relatively high $K_{1/2-\text{CO}_2}$ ranging from ~ 6 to $60 \mu\text{M}$ (more specifically, heterokont and haptophyte algae: $31\text{--}59 \mu\text{M}$; green algae: $12\text{--}38 \mu\text{M}$; haptophyte algae: $6\text{--}22 \mu\text{M}$; Badger et al., 1998; Badger and Bek, 2008), which implies that, for many algal species, Rubisco is below half saturation at modern seawater $\text{CO}_{2\text{aq}}$ concentrations of $10\text{--}30 \mu\text{M}$ (Giordano et al., 2005). Flux models suggest that unless algae are able to actively transport inorganic carbon, CO_2 limitation would be widespread in the modern ocean. This would be particularly true for larger cells with low affinities for CO_2 (Riesbesell et al. (1993); Reinfelder, 2011).

It is now known that most algae have strategies to actively increase intracellular CO_2 concentrations (Coleman et al., 2002), mediated by carbon concentrating mechanisms (CCMs). Intracellular carbon concentrations 80 times ambient levels can be associated with CCMs (Badger et al., 1998), resulting from the release of a carbonic anhydrase that drives the dehydration of HCO_3^- to $\text{CO}_{2\text{aq}}$, direct uptake of HCO_3^- or $\text{CO}_{2\text{aq}}$, or some combination of each (Coleman et al., 2002).

Upregulation of a CCM will have isotopic consequences that impact the expression of ϵ_p . Aside from altering the magnitude of intracellular CO_2 through enhancement of external $\text{CO}_{2\text{aq}}$ or active transport, the transport of HCO_3^- alters the isotopic composition of the intracellular carbon pool given that the $\delta^{13}\text{C}$ value of bicarbonate is $\sim 10\%$ more positive relative to $\text{CO}_{2\text{aq}}$ (at 25°C). Growth rate also becomes independent of ambient CO_2 concentrations because the organism is in physical control of CO_2 supply. Isotopic evidence for active uptake was first observed in chemostat experiments of the diatom *P. tricornutum* (Laws et al., 1997). In this experiment, ϵ_p was shown to be nonlinear with respect to μ/CO_2 (Figure 13), and argued to reflect the influence of actively transported carbon as $[\text{CO}_{2\text{aq}}]$ became limited by diffusion flux (Cassar et al., 2002; Laws et al., 1997).

Haptophyte species have also been studied for the influence of nondiffusive CO_2 flux. Active uptake of carbon has been implicated from cultures that show irradiance effects (Rost et al., 2002), nonlinear behavior between ϵ_p and μ/CO_2 (Riesbesell et al., 2000; Figure 6), and cultures (Rickaby et al., 2010; Figure 8) and field data (Benthien et al., 2002) that

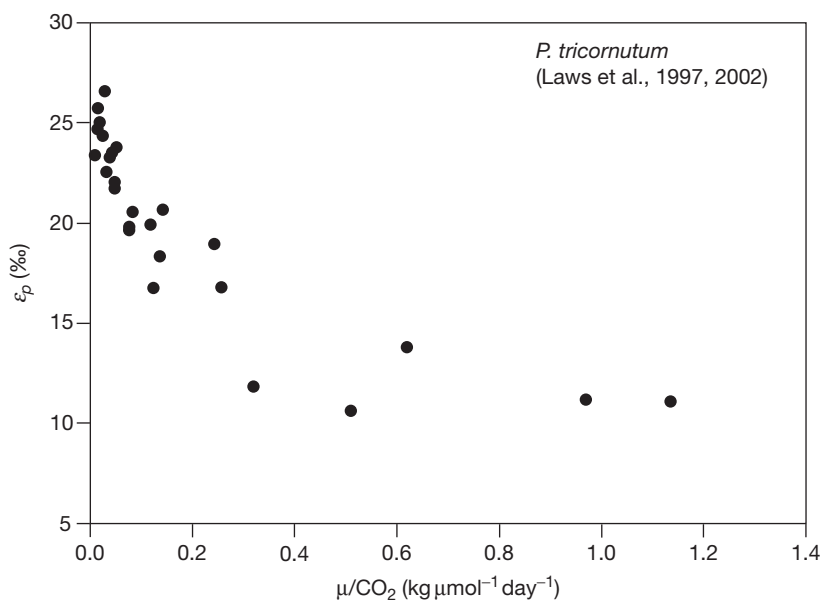


Figure 13 Extended data for diatom *P. tricornutum* from Laws et al. (1997). Reproduced from Laws EA, Popp BN, Cassar N, and Tanimoto J (2002) ^{13}C discrimination patterns in oceanic phytoplankton: Likely influence of CO_2 concentrating mechanisms, and implications for palaeoreconstructions. *Functional Plant Biology* 29: 323–333.

show a positive correspondence between ε_p and $1/\text{CO}_2$ contrary to diffusion theory. Higher-than-ambient intracellular CO_2 concentrations have been measured in *E. huxleyi* and *I. galbana* (Burns and Beardall, 1987; Sekino and Shiraiwa, 1994) and bicarbonate appears to be a major source of carbon for photosynthesis (Buitenhuis et al., 1999; Nimer and Merrett, 1992; Nimer and Merrett, 1993; Paasche, 1964; Sekino and Shiraiwa, 1994). Some haptophytes seem to have an inefficient inorganic carbon pump and only little carbonic anhydrase activity (Sekino and Shiraiwa, 1994; Sekino et al., 1996), although Herfort et al. (2002) provide evidence that bicarbonate anion exchange proteins are present and active in *E. huxleyi*. Other studies find inducible external carbonic anhydrase activity and subsequent CO_2 diffusion in *P. globosa* and *E. huxleyi* (Elzenga et al., 2000; Herfort et al. (2002). Calcification is also argued to help increase intracellular $[\text{CO}_{2\text{aq}}]$ through proton production and dehydration of intracellular bicarbonate (Nimer and Merrett, 1993; Sekino and Shiraiwa, 1994).

Use of HCO_3^- through conversion by external carbonic anhydrase or H^+ production during calcification is not expected to contribute isotope effects beyond altering the flux of $\text{CO}_{2\text{aq}}$ (Laws et al., 2002) and no isotopic differences were found between calcifying and noncalcifying stains of *E. huxleyi* in chemostat incubations (Bidigare et al., 1997).

12.13.4.1 Models for Active Carbon Uptake

$\text{CO}_{2\text{aq}}$ and the Calvin cycle is the dominant carbon fixation pathway for *E. huxleyi*, although β -carboxylases and reactions are also in operation to some extent (Tsuji et al., 2009) with clear differences in the mode of carbon supply and affinity to CO_2 among haptophytes (Badger et al., 1998). How these differences evolved through time and whether or not CCMs were an important aspect of ancient alkenone producers

remains speculative. Whereas some organisms, such as diatoms, show highly efficient and active CCMs (Badger et al., 1998; Raven and Johnston, 1991), CCMs in *E. huxleyi* and other coccolithophores appear weakly expressed (Bidigare et al., 1997; Rickaby et al., 2010). *E. huxleyi* originated during the Pleistocene under some of the lowest CO_2 levels of the past 50 My. *G. oceanica*, with a distinctly different physiological behavior (Rickaby et al., 2010; Figure 8), originated 2 Ma under similarly low CO_2 conditions. Physiological parameters of more ancient alkenone producers are simply unknown. It is possible that ancient haptophytes had inefficient or a lack of CCMs under the much higher CO_2 levels of the past (Henderiks and Pagani, 2008). However, if active carbon transport was an important and widespread physiological characteristic, then upregulation of CCMs could have been responsible for the decrease in ε_p values near the Oligocene–Eocene boundary in response to low CO_2 thresholds, or to simply a decline in atmospheric CO_2 (Figures 1 and 11). If that was the case, quantitative reconstructions of $p\text{CO}_2$ would be compromised.

Active carbon transport models need to account for both diffusion flux and active $\text{CO}_{2\text{aq}}$ or HCO_3^- uptake and several models have been developed to describe resulting isotope effects (Burkhardt et al., 1999a; Francois et al., 1993; Keller and Morel, 1999; Laws et al., 1997; Sharkey and Berry, 1985).

Sharkey and Berry (1985) described isotope fractionation in terms of HCO_3^- uptake and carbon leakage (the ratio of the diffusive carbon flux out of the cell to the flux into the cell):

$$\varepsilon_p = \varepsilon_{b-c} + \varepsilon_f \frac{F_{\text{out}}}{F_{\text{in}}} \quad [17]$$

where ε_{b-c} is the temperature-dependent equilibrium isotope fractionation between $\text{CO}_{2\text{aq}}$ and HCO_3^- . Because Sharkey and Berry (1985) assumed only bicarbonate uptake, Burkhardt et al.

(1999a) expanded the model to include multiple carbon sources (i.e., CO_2 diffusion flux and active HCO_3^- influx):

$$\varepsilon_p = a\varepsilon_{b-c} + \varepsilon_f \frac{F_{\text{out}}}{F_{\text{in}} + F_{\text{HCO}_3^-}} \quad [18]$$

where a is the fractional component of HCO_3^- relative to the total carbon uptake. Here, ε_p decreases with increasing contributions of actively transported HCO_3^- and/or as the rate of intracellular carbon leakage decreases. Eqn [18] can also be cast in terms of carbon-specific growth rate (μ_c) or the carboxylation rate (F_2) considering $F_2 = (F_{\text{in}} + F_{\text{HCO}_3^-}) - F_{\text{out}}$. Substitution leads to:

$$\varepsilon_p = a\varepsilon_{b-c} + \varepsilon_f - \varepsilon_f \left(\frac{\mu_c}{F_{\text{in}} + F_{\text{HCO}_3^-}} \right) \quad [19]$$

Recasting carbon fluxes in terms of μ defines isotope fractionation in more tangible and measurable variables, but questions persist as to the levels of stress that trigger active bicarbonate (or $\text{CO}_{2\text{aq}}$) uptake. Low membrane permeabilities and the transport of charged anions require upregulation of CCMs to be energy expensive (Raven, 1997). One perspective assumes that active transport occurs when diffusive flux achieves a minimum threshold of intracellular CO_2 necessary for adequate growth. Minimum diffusive flux estimates depend on ambient $[\text{CO}_{2\text{aq}}]$ and constraints imposed by cell geometry. Assuming spherical geometry, minimum $[\text{CO}_{2\text{aq}}]$ that provides an adequate carbon flux can be defined as (Burkhardt et al., 1999a,b; Riebesell et al., 1993; Wolf-Gladrow and Riebesell, 1997)

$$[\text{CO}_2]_{\text{min}} = \frac{F_{\text{in}}}{4\pi r D(1 + r_s/r_k)} \quad [20]$$

where D is the diffusion coefficient of CO_2 , r_s is the 'surface area equivalent' spherical cell radius for spheroids (Wolf-Gladrow and Riebesell, 1997), r_k is the reacto-diffusive length (i.e., length of the boundary layer where HCO_3^- has the opportunity to convert to $\text{CO}_{2\text{aq}}$), and the term $(1 + r_s/r_k)$ represents the contribution of extracellular, uncatalyzed $\text{HCO}_3^- - \text{CO}_{2\text{aq}}$ conversion to the total supply of CO_2 (Burkhardt et al., 1999a,b). Other models of active transport derive from the model of diffusive transport derived for terrestrial photosynthesis (i.e., eqn [3]) and also impose flux constraints determined by cell size and shape. The model proposed by Laws et al. (1997, 2002) assumes transport by both diffusion and active uptake in order to describe the nonlinear culture results of *P. tricornutum* (Figure 13):

$$\varepsilon_p = \varepsilon_f + \varepsilon_t - \varepsilon_{-t} - \left(\frac{1}{1 + \frac{C_e P}{\mu C(1+\beta)}} \right) \left(\frac{\varepsilon_f - \varepsilon_{-t}}{\beta + 1} \right) \quad [21]$$

Here, β is a constant equivalent to the ratio of CO_2 loss (leakage by diffusion) to carbon fixation. As detailed in Laws et al. (2002), the value of ε_p becomes insensitive to μ/CO_2 when

$$\frac{\mu}{C_e} \geq \frac{P}{C(1+\beta)} \quad [22]$$

Using reasonable relationships between membrane permeability and carbon content, $P/C = 0.285/r$, where r is the radius of the cell. Minimum $[\text{CO}_{2\text{aq}}]$ that would trigger active transport occurs when the term $(1 + \beta)$ approaches unity, or leakage

is zero. Laws et al. (2002) calculate that ε_p for *E. huxleyi* would become a nonlinear function of μ/CO_2 as photoperiod growth rate exceeds 1.1 day^{-1} for a cell radius of $2.6 \mu\text{m}$, dimensions appropriate for modern *E. huxleyi* (Popp et al., 1998a).

Photoperiod growth rates in the natural environment for *E. huxleyi* and other alkenone-producing haptophytes are typically below 1 day^{-1} , ranging from 0.1 to 1 day^{-1} with the highest rates associated with the Peru upwelling zone (Bidigare et al., 1997; Popp et al., 2006). Cell dimensions of alkenone-producing algae for the past $\sim 45 \text{ My}$ (Henderiks and Pagani, 2007, 2008), in conjunction with estimates of $p\text{CO}_2$ (assuming changes in cell geometry do not exert significant impact on the magnitude of $p\text{CO}_2$), provide a means to identify geologic intervals when upregulation of CCMs was potentially necessary. For example, cell radii for alkenone producers range from ~ 4 to $2.4 \mu\text{m}$ across the Eocene/Oligocene boundary (Henderiks and Pagani, 2008) as $[\text{CO}_{2\text{aq}}]$ presumably fell from ~ 30 to $\sim 20 \mu\text{m}$ (Pagani et al., 2011), and cell radii were about 50% smaller during the Early Miocene (Henderiks and Pagani, 2007) when $[\text{CO}_{2\text{aq}}]$ appears similar to today. Knowledge of cell radius allows calculation of the ratio P/C (Laws et al., 2002) and the ratio μ/C_e can be estimated from paleo- CO_2 reconstructions and a range of modern haptophyte growth rates, assuming paleo- CO_2 estimates are valid (even if CCMs were active). Figure 14 shows that for low to moderate growth rates, upregulation of CCMs is anticipated during the Miocene, and particularly during the climatic optimum of the Late-Early Miocene, suggesting that the alkenone- CO_2 proxy could be compromised during these times and Zhang et al. (in press) insensitive to changes in atmospheric $p\text{CO}_2$. Therefore, it is possible that relatively invariant alkenone-based $p\text{CO}_2$ records during the Early Miocene (Pagani et al., 1999) reflect the influence of CCMs. Obviously, this result is speculative given the necessary assumptions. For example, CO_2 concentrations used in this exercise are derived from alkenone measurements and if CCMs were active, then these alkenone-based CO_2 values would appear artificially lower than actual concentrations and further exaggerate the potential influence of CCMs. Regardless, determining the activity of CCMs through time will be an important step in better understanding the capacity of the alkenone- CO_2 methodology to accurately determine ancient CO_2 levels, and the approach explored here will need to be more rigorously tested to determine its utility.

12.13.5 Summary

This chapter attempts to frame the capacities and limitations of the alkenone- CO_2 to help advance its progress and utility. The alkenone CO_2 proxy remains one of the few techniques that allows qualitative and potentially quantitative $p\text{CO}_2$ reconstructions over the past $\sim 45 \text{ My}$. The methodology, founded on the carbon isotopic composition of alkenones, requires consideration of growth effects related to nutrients and irradiance, cell size evolution, and the capacity of alkenone producers to deviate from a simple diffusive model of carbon uptake over time and space. Determining the role and activity of active transport mechanisms (CCMs) embedded in alkenone isotopic signals over long-time scales will be a

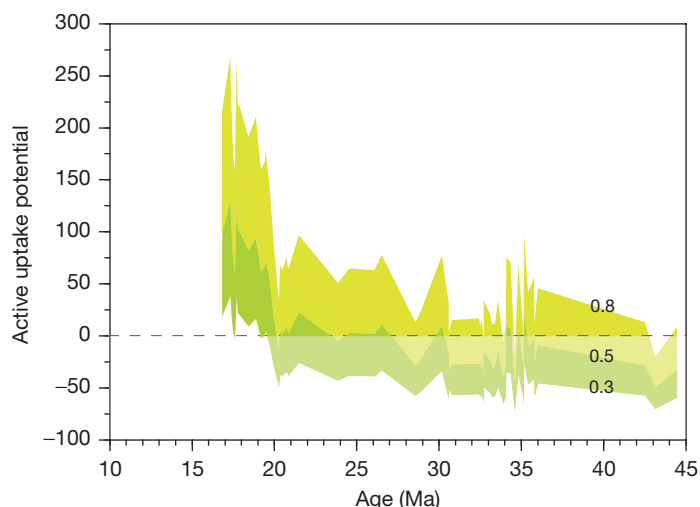


Figure 14 The potential for upregulation of CCMs over geologic time. Calculations assume a range of potential 24-h averaged growth rates; 0.3, 0.5, and 0.8 day^{-1} . Active uptake potential $([(\mu/C_p)/(P/C)]100-100)$ represents an arbitrary, qualitative scale of CCM activity. Modified from Zhang YG, Pagani M, Liu Z, Bohaty SM, DeConto R (in press) A 40-million-year history of atmospheric CO_2 . *Philosophical Transactions of the Royal Society B*.

critical step forward in determining the veracity of reconstructed $p\text{CO}_2$.

Improvements in the alkenone CO_2 proxy as well as temperature and nutrient estimates will help provide us with quantitative estimates of Earth climate sensitivity in the geologic past. Such estimates shape our understanding of Earth's climate history, as well as our perspective on what we will face in the near future under rising levels of atmospheric carbon dioxide.

References

- Arthur MA, Walter DE, and Claypool GE (1985) Anomalous ^{13}C enrichment in modern marine organic carbon. *Nature* 315: 216–218.
- Badger MR, Andrews TJ, Whitney SM, et al. (1998) The diversity and coevolution of Rubisco, plastids, pyrenoids, and chloroplast-based CO_2 -concentrating mechanisms in algae. *Canadian Journal of Botany* 76: 1052–1071.
- Badger MR and Bek EJ (2008) Multiple Rubisco forms in proteobacteria: Their functional significance in relation to CO_2 acquisition by the CBB cycle. *Journal of Experimental Botany* 59: 1525–1541.
- Barron EJ and Washington WM (1985) Warm Cretaceous climates: High atmospheric CO_2 as a plausible mechanism. *The Carbon Cycle and Atmospheric CO_2 : Natural Variations Archean to Present. Geophysical Monograph*, vol. 32, pp. 546–553. Washington, DC: AGU.
- Benthien A, Andersen N, Schulte S, Müller P, Schneider R, and Wefer G (2002) Carbon isotopic composition of the C37:2 alkenone in core top sediments of the South Atlantic Ocean: Effects of CO_2 and nutrient concentrations. *Global Biogeochemical Cycles* 16(1): 1012.
- Benthien A, Zondervan I, Engel A, Hefter J, Terbrüggen A, and Riebesell U (2007) Carbon isotopic fractionation during mesocosm bloom experiment dominated by *Emiliania huxleyi*: Effects of CO_2 concentration and primary production. *Geochimica et Cosmochimica Acta* 71: 1528–1541.
- Berner RA (1991) A model for atmospheric CO_2 over the Phanerozoic time. *American Journal of Science* 291: 339–376.
- Bidigare RR, Fluegge A, Freeman KH, et al. (1997) Consistent fractionation of ^{13}C in nature and in the laboratory: Growth-rate effects in some haptophyte algae. *Global Biogeochemical Cycles* 11: 279–292.
- Bidigare RR, Fluegge A, Freeman KH, et al. (1999) Correction to 'Consistent fractionation of ^{13}C in nature and in the laboratory: Growth-rate effects in some haptophyte algae' by Bidigare et al. 1997. *Global Biogeochemical Cycles* 13: 251.
- Bijl PK, Houben AJP, Schouten S, et al. (2010) Transient middle Eocene atmospheric CO_2 and temperature variations. *Nature* 330: 819–821.
- Burkhardt S, Riebesell U, and Zondervan I (1999a) Effects of growth rate, CO_2 concentration, and cell size on the stable carbon isotope fractionation in marine phytoplankton. *Geochimica et Cosmochimica Acta* 63: 3729–3741.
- Burkhardt S, Riebesell U, and Zondervan I (1999b) Stable carbon isotope fractionation by marine phytoplankton in response to daylength, growth rate, and CO_2 availability. *Marine Ecology Progress Series* 184: 31–41.
- Burns BD and Beardall J (1987) Utilization of inorganic carbon by marine microalgae. *Journal of Experimental Marine Biology and Ecology* 107(1): 75–86.
- Calder JA and Parker PL (1973) Geochemical implications of induced changes in C^{13} fractionation by blue-green algae. *Geochimica et Cosmochimica Acta* 37: 133–140.
- Cassar N, Laws EA, and Popp BN (2006) Carbon isotopic fractionation by the marine diatom *Phaeodactylum tricornutum* under nutrient- and light-limited growth conditions. *Geochimica et Cosmochimica Acta* 70: 5323–5335.
- Cassar N, Laws EA, Popp BN, and Bidigare RR (2002) Inorganic carbon for photosynthesis in a strain of *Phaeodactylum tricornutum*. *Limnology and Oceanography* 47: 1192–1197.
- Clark DR and Flynn KJ (2000) The relationship between the dissolved inorganic carbon concentration and growth rate in marine phytoplankton. *Proceedings of the Royal Society of London, Series B: Biological Sciences* 267: 953–959.
- Coleman B, Huertas IE, Bhatti S, and Dason JS (2002) The diversity of inorganic carbon acquisition mechanisms in eukaryotic microalgae. *Functional Plant Biology* 29: 261–270.
- Conte M, Volkman J, and Eglinton G (1994) Lipid biomarkers of the haptophyta. In: Green JC and Leadbeater BSC (eds.), *The Haptophyte Algae*, pp. 351–371. Oxford: Clarendon Press.
- Dean WE, Arthur MA, and Claypool GE (1986) Depletion of ^{13}C in cretaceous marine organic matter: Source, diagenetic, or environmental signal? *Marine Geology* 70: 119–157.
- Degens ET, Behrendt M, Gotthardt B, and Reppman E (1968a) Metabolic fractionation of carbon isotopes in marine plankton – II. Data on samples collected off the coasts of Peru and Ecuador. *Deep Sea Research* 15: 12–20.
- Degens ET, Guillard RRL, Sackett WM, and Hellebust JA (1968b) Metabolic fractionation of carbon isotopes in marine plankton – I. Temperature and respiration experiments. *Deep Sea Research* 15: 1–9.
- DeNiro MJ and Epstein S (1977) Mechanism of carbon isotope fraction associated with lipid synthesis. *Science* 197: 261–263.
- Des Marais DJ, Mitchell JM, Meinschein WG, and Hayes JM (1980) The carbon isotope biogeochemistry of the individual hydrocarbons in bat guano and the ecology of the insectivorous bats in the region of Carlsbad, New Mexico. *Geochimica et Cosmochimica Acta* 44: 2075–2086.
- Deuser WG, Degens ET, and Guillard RR (1968) Carbon isotope relationships between plankton and sea water. *Geochimica et Cosmochimica Acta* 32: 657–660.
- Eek ME, Whiticar MJ, Bishops JKB, and Wong CS (1999) Influence of nutrients on carbon isotope fractionation by natural populations of Pymnesiophyte algae in NE Pacific. *Deep Sea Research Part II: Topical Studies in Oceanography* 46: 2863–2876.

- Elzenga J, Prins H, and Stefels J (2000) The role of extracellular carbonic anhydrase activity in inorganic ^{12}C carbon utilization of *Phaeocystis globosa* (Prymnesiophyceae): A comparison with other marine algae using the isotopic disequilibrium technique. *Limnology and Oceanography* 45(2): 372–380.
- Emerson S, Stump C, Grootes PM, Stuiver M, Fatwell G, and Schmidt F (1987) Estimates of degradable organic carbon in deep-sea surface sediments from ^{14}C concentrations. *Nature* 329: 51–53.
- Epstein BL, D'Hondt S, and Hargraves PE (2001) The possible metabolic role of C_{37} alkenones in *Emiliania huxleyi*. *Organic Geochemistry* 32: 867–875.
- Falkowski PG (1991) Species variability in the fractionation of ^{12}C and ^{13}C by marine phytoplankton. *Journal of Plankton Research* 13: 21–281.
- Farquhar GD, Ehleringer JR, and Hubick KT (1989) Carbon isotope discrimination and photosynthesis. *Annual Review of Plant Physiology and Plant Molecular Biology* 40: 503–537.
- Farquhar GD, O'Leary MHB, and Berry JA (1982) On the relationship between carbon isotope discrimination and the intercellular carbon dioxide concentration in leaves. *Australian Journal of Plant Physiology* 9: 121–137.
- Francois R, Allabet MA, Goericke R, McCorkle DC, Brunet C, and Poisson A (1993) Changes in the $\delta^{13}C$ of surface water particulate organic matter across the subtropical convergence in the SW Indian Ocean. *Global Biogeochemical Cycles* 7: 627–644.
- Freeman KH and Hayes JM (1992) Fractionation of carbon isotopes by phytoplankton and estimates of ancient CO_2 levels. *Global Biogeochemical Cycles* 6: 185–198.
- Freeman KH, Hayes JM, Trendel J-M, and Albrecht P (1990) Evidence from carbon isotopes measurements for diverse origins of sedimentary hydrocarbons. *Nature* 343: 254–256.
- Freeman KH and Pagani M (2005) Alkenone-based estimates of past CO_2 levels: A consideration of their utility based on an analysis of uncertainties. In: Ehleringer JR, Cerling TE, and Dearing MD (eds.) *A History of Atmospheric CO_2 and its Effects on Plants, Animals, and Ecosystems*. Ecological Studies, vol. 177, p. 530. New York: Springer.
- Giordano M, Beardall J, and Raven JA (2005) CO_2 concentrating mechanisms in algae: Mechanisms, environmental modulation, and evolution. *Annual Review of Plant Biology* 56: 99–131.
- Goericke R, Montoya JP, and Fry B (1994) Physiology of isotope fractionation in algae and cyanobacteria. In: Lajtha K and Michener B (eds.) *Stable Isotope in Ecology*. Cambridge: Blackwell.
- Guy RD, Fogel ML, and Berry JA (1993) Photosynthetic fractionation of the stable isotopes of oxygen and carbon. *Plant Physiology* 101: 37–47.
- Hay W (1977) *Calcareous nannofossils*. In: Ramsay A (ed.), *Oceanic Micropaleontology*, vol. 2, pp. 1055–1200. London: Academic Press.
- Hayes JM (1993) Factors controlling ^{13}C contents of sedimentary organic compounds: Principles and evidence. *Marine Geology* 113: 111–125.
- Hayes JM, Popp BN, Takigiku R, and Johnson MW (1989) An isotopic study of biogeochemical relationships between carbonates and organic carbon in the Greenhorn Formation. *Geochimica et Cosmochimica Acta* 53: 2961–2972.
- Hayes JM, Strauss H, and Kaufman AJ (1999) The abundance of ^{13}C in marine organic matter and isotopic fractionation in the global biogeochemical cycle of carbon during the past 800 Ma. *Chemical Geology* 161: 103–125.
- Hayes JM, Takigiku R, Ocampo R, Callot HJ, and Albrecht P (1987) Isotopic compositions and probable origins of organic molecules in the Eocene Messel Shale. *Nature* 329: 48–51.
- Henderiks J and Pagani M (2007) Refining ancient carbon dioxide estimates: Significance of coccolithophore cell size for alkenone-based pCO_2 records. *Paleoceanography* 22: <http://dx.doi.org/10.1029/2006PA001399>.
- Henderiks J and Pagani M (2008) Coccolithophore cell size and the Paleogene decline in atmospheric CO_2 . *Earth and Planetary Science Letters* 269: 575–583.
- Herfort L, Thake B, and Roberts J (2002) Acquisition and use of bicarbonate by *Emiliania huxleyi*. *New Phytology* 156: 427–436.
- Hinga K, Arthur M, Pilson M, and Whitaker D (1994) Carbon isotope fractionation by marine phytoplankton in culture: The effects of CO_2 concentration, pH, temperature, and species. *Global Biogeochemical Cycles* 8(1): 91–102.
- Hollander DJ and McKenzie JA (1991) CO_2 control on carbon isotope fractionation during aqueous photosynthesis: A paleo- pCO_2 barometer. *Geology* 19: 929–932.
- Iglesias-Rodríguez MD, Halloran PR, Rickaby REM, et al. (2008) Phytoplankton calcification in a high- CO_2 world. *Science* 320: 336–340.
- Jasper JP and Hayes JM (1990) A carbon isotope record of CO_2 levels during the late Quaternary. *Nature* 347: 462–464.
- Jasper JP, Hayes JM, Mix AC, and Prah FG (1994) Photosynthetic fractionations of ^{13}C and concentrations of dissolved CO_2 in the central equatorial Pacific during the last 255,000 years. *Paleoceanography* 9: 781–798.
- Kaplan A and Reinhold L (1999) CO_2 concentrating mechanisms in photosynthetic microorganisms. *Annual Review of Plant Physiology and Plant Molecular Biology* 50: 539–570.
- Keller K and Morel F (1999) A model of carbon isotopic fractionation and active carbon uptake in phytoplankton. *Marine Ecology Progress Series* 182: 295–298.
- Laws EA, Bidigare RR, and Popp BN (1997) Effect of growth rate and CO_2 concentration on carbon isotopic fractionation by the marine diatom *Phaeodactylum tricornutum*. *Limnology and Oceanography* 42: 1552–1560.
- Laws EA, Popp BN, Bidigare RR, Riebesell U, Burkhardt S, and Wakeham SG (2001) Controls on the molecular distribution and carbon isotopic composition of alkenones in certain haptophyte algae. *Geochemistry, Geophysics, Geosystems* 2: <http://dx.doi.org/10.1029/2000GC000057>.
- Laws EA, Popp BN, Bidigare RR, Kennicut MC, and Macko SA (1995) Dependence of phytoplankton carbon isotopic composition on growth rate and $[CO_2]_{aq}$: Theoretical considerations and experimental results. *Geochimica et Cosmochimica Acta* 59: 1131–1138.
- Laws EA, Popp BN, Cassar N, and Tanimoto J (2002) ^{13}C discrimination patterns in oceanic phytoplankton: Likely influence of CO_2 concentrating mechanisms, and implications for palaeoreconstructions. *Functional Plant Biology* 29: 323–333.
- Marlowe IT, Brassell SC, Eglinton G, and Green JC (1990) Long-chain alkenones and alkyl alkenoates and the fossil coccolith record of marine sediments. *Chemical Geology* 88: 349–375.
- Marlowe IT, Green JC, Neal AC, Brassell SC, Eglinton G, and Course PA (1984) Long chain (n -C37-C39) alkenones in the Prymnesiophyceae. Distribution of alkenones and other lipids and their taxonomic significance. *British Phycology Journal* 19: 203–216.
- Martin CL and Tortell PD (2006) Bicarbonate transport and extracellular carbonic anhydrase activity in Bering Sea phytoplankton Assemblages: Results from isotope disequilibrium experiments. *Limnology and Oceanography* 51: 2111–2121.
- Matsuda Y, Hara T, and Colman B (2001) Regulation of the induction of bicarbonate uptake by dissolved CO_2 in the marine diatom, *Phaeodactylum tricornutum*. *Plant, Cell and Environment* 24: 611–620.
- Matthews DE and Hayes JM (1978) Isotope-ratio-gas chromatography mass-spectrometry. *Analytical Chemistry* 50: 1465–1473.
- Maynard JB (1981) Carbon isotopes as indicators of dispersal patterns in Devonian–Mississippian shales of the Appalachian Basin. *Geology* 9: 262–265.
- McCabe B (1985) *The Dynamics of ^{13}C in Several New Zealand lakes*. PhD Thesis, University of Waikato, Hamilton, New Zealand, pp. 278.
- McNevin DB, Badger MR, Kane HJ, and Farquhar GD (2006) Measurement of (carbon) kinetic isotope effect by Rayleigh fractionation using membrane inlet mass spectrometry for CO_2 -consuming reactions. *Functional Plant Biology* 33: 1115–1128.
- Nimer N and Merrett M (1992) Calcification and utilization of inorganic carbon by the coccolithophorid *Emiliania huxleyi* Lohmann. *New Phytologist* 121(2): 173–177.
- Nimer NA and Merrett MJ (1993) Calcification rate in *Emiliania huxleyi* Lohmann in response to light, nitrate and availability of inorganic carbon. *New Phytologist* 123: 673–677.
- Nimer NA and Merrett MJ (1996) The development of a CO_2 -concentrating mechanism in *Emiliania huxleyi*. *New Phytologist* 133: 383–389.
- Paasche E (1964) A tracer study of the inorganic carbon uptake during coccolith formation and photosynthesis in the coccolithophorid *Coccolithus huxleyi*. *Phytologia Plantarum* Suppl. 3: 5–82.
- Pagani M (2002) The alkenone- CO_2 proxy and ancient atmospheric CO_2 . In: Gröcke DR and Kucera M (eds.) *Understanding Climate Change: Proxies, Chronology, and Ocean–Atmosphere Interactions*, *Philosophical Transactions of the Royal Society of London*. Series A360: 575–802.
- Pagani M, Arthur MA, and Freeman KH (1999) Miocene evolution of atmospheric carbon dioxide. *Paleoceanography* 14: 273–292.
- Pagani M, Arthur MA, and Freeman KH (2000) Variations in Miocene phytoplankton growth rates in the southwest Atlantic: Evidence for changes in ocean circulation. *Paleoceanography* 15: 486–496.
- Pagani M, Freeman KH, Ohkouchi K, and Caldeira K (2002) Comparison of water column $[CO_2]_{aq}$ with sedimentary alkenone-based estimates: A test of the alkenone- CO_2 proxy. *Paleoceanography* 17: 1069. <http://dx.doi.org/10.1029/2002PA000756>.
- Pagani M, Huber M, Liu Z, et al. (2011) The role of carbon dioxide during the onset of Antarctic glaciation. *Science* 334: 1261–1264.
- Pagani M, Liu Z, LaRiviera J, and Ravelo AC (2009) High climate sensitivity to atmospheric carbon dioxide for the past 5 million years. *Nature Geoscience* 3: 27–30.
- Pagani M, Zachos J, Freeman KH, Bohaty S, and Tipler B (2005) Marked decline in atmospheric carbon dioxide concentrations during the Paleogene. *Science* 309: 600–603.
- Pardue JW, Scalani RS, Van Baalen C, and Parker PL (1976) Maximum carbon isotope fractionation in photosynthesis by blue-green algae and a green alga. *Geochimica et Cosmochimica Acta* 40: 309–312.
- Park R and Epstein S (1961) Metabolic fractionation of C_{13} and C_{12} in plants. *Plant Physiology* 36: 133–138.

- Popp BN, Bidigare RR, Deschenes B, et al. (2006) A new method for estimating growth rates of alkenone-producing haptophytes. *Limnology and Oceanography: Methods* 4: 114–129.
- Popp BN, Hanson KL, Dore JE, Bidigare RR, Laws EA, and Wakeham SG (1999) Controls on the carbon isotopic composition of phytoplankton: Paleooceanographic perspectives. In: Abrantes F and Mix A (eds.) *Reconstructing Ocean History: A Window into the Future*. New York: Plenum.
- Popp BN, Kenig F, Wakeham SG, Laws EA, and Bidigare RR (1998a) Does growth rate affect ketone unsaturation and intracellular carbon isotopic variability in *Emiliania huxleyi*? *Paleoceanography* 13: 35–41.
- Popp BN, Laws EA, Bidigare RR, Dore JE, Hanson KL, and Wakeham SG (1998b) Effect of phytoplankton cell geometry on carbon isotopic fractionation. *Geochimica et Cosmochimica Acta* 62: 69–77.
- Popp BN, Takigiku R, Hayes JM, Louda JW, and Baker EW (1989) The post-Paleozoic chronology and mechanism of ^{13}C depletion in primary marine organic matter. *American Journal of Science* 289: 436–454.
- Prahl FG and Wakeham SG (1987) Calibration of unsaturation patterns in long-chain ketone compositions for paleotemperature assessment. *Nature* 330: 367–369.
- Prahl FG, Wolfe GV, and Sparrow MA (2003) Physiological impacts on alkenone paleothermometry. *Paleoceanography* 18: 1025. <http://dx.doi.org/10.1029/2002PA000803>.
- Rau G, Riebesell U, and Wolf-Gladrow D (1996) A model of photosynthetic ^{13}C fractionation by marine phytoplankton based on diffusive molecular CO_2 uptake. *Marine Ecology-Progress Series* 133: 275–285.
- Rau G, Takahashi T, Des Marais D, Repeta D, and Martin J (1992) The relationship between $\delta^{13}C$ of organic matter and $[CO_2]_{aq}$ in ocean surface water: Data from a JGOFS site in the northeast Atlantic Ocean and a model. *Geochimica et Cosmochimica Acta* 56(3): 1413–1419.
- Rau GH, Froelich PN, Takahashi T, and Des Marais DJ (1991) Does sedimentary organic $\delta^{13}C$ record variation in Quaternary ocean $[CO_2]_{aq}$. *Paleoceanography* 6: 335–347.
- Rau GH, Sweeney RE, and Kaplan IR (1982) Plankton $^{13}C:^{12}C$ ratio changes with latitude: Differences in northern and southern oceans. *Deep Sea Research* 29: 1035–1039.
- Rau GH, Takahashi T, and Des Marais DJ (1989) Latitudinal variation in plankton $\delta^{13}C$: Implications for CO_2 and productivity in past oceans. *Nature* 341: 516–518.
- Raven J (1997) Inorganic carbon acquisition by marine autotrophs. *Advances in Botanical Research* 27: 85–209.
- Raven JA, Cockell CS, and De La Rocha CL (2008) The evolution of inorganic carbon concentrating mechanisms in photosynthesis. *Philosophical Transactions of the Royal Society B: Biological Sciences* 363: 2641–2650.
- Raven J, Giordano M, Beardall J, and Maberly SC (2011) Algal and aquatic plant carbon concentrating mechanisms in relation to environmental change. *Photosynthesis Research* 1–16: <http://dx.doi.org/10.1007/s11120-011-9632-6>.
- Raven JA and Johnston AM (1991) Mechanisms of inorganic-carbon acquisition in marine phytoplankton and their implications for the use of other resources. *Limnology and Oceanography* 36: 1701–1714.
- Raymo ME, Grant B, Horowitz M, and Rau GH (1996) Mid-Pliocene warmth: Stronger greenhouse and stronger conveyor. *Marine Micropaleontology* 27: 313–326.
- Reinfeider JR (2011) Carbon concentrating mechanisms in eukaryotic marine phytoplankton. *Annual Review of Marine Science* 3: 291–315.
- Rickaby R, Henderiks J, and Young J (2010) Perturbing phytoplankton: Response and isotopic fractionation with changing carbonate chemistry in two coccolithophore species. *Climate of the Past* 6: 771–785.
- Riebesell U, Revill A, Holdsworth D, and Volkman J (2000) The effects of varying CO_2 concentration on lipid composition and carbon isotope fractionation in *Emiliania huxleyi*. *Geochimica et Cosmochimica Acta* 64(24): 4179–4192.
- Riebesell U, Wolf-Gladrow DA, and Smectacek V (1993) Carbon dioxide limitation of marine phytoplankton growth rates. *Nature* 361: 249–251.
- Robinson JJ, Scott KM, Swanson ST, et al. (2003) Kinetic isotope effect and characterization of form II RubisCO from the chemoautotrophic endosymbionts of the hydrothermal vent tubeworm *Riftia pachyptila*. *Limnology and Oceanography* 48: 48–54.
- Roeske CA and O'Leary MH (1984) Carbon isotope effect in the enzyme-catalyzed carboxylation of ribulose biphosphate. *Biochemistry* 23: 6275–6285.
- Rost B and Riebesell U (2004) Coccolithophores and the biological pump: Responses to environmental changes. In: Thierstein HR and Young JR (eds.) *Coccolithophores – From Molecular Processes to Global Impact*, pp. 76–99. New York: Springer.
- Rost B, Riebesell U, and Sültemeyer D (2006) Carbon acquisition of marine phytoplankton: Effect of photoperiod length. *Limnology and Oceanography* 51: 12–20.
- Rost B, Zondervan I, and Riebesell U (2002) Light-dependent carbon isotope fractionation in the coccolithophorid *Emiliania huxleyi*. *Limnology and Oceanography* 47(1): 120–128.
- Sackett WM (1986) $\delta^{13}C$ signatures of organic carbon in southern high latitudes deep sea sediments; paleotemperature implications. *Organic Geochemistry* 9: 63–68.
- Sackett WM, Eckelmann WR, Bender ML, and Bé AWH (1965) Temperature dependence of carbon isotope composition in marine plankton and sediments. *Science* 148: 235–237.
- Schouten S, Klein Breteler WCM, Blokker P, et al. (1998) Biosynthetic effects on the stable carbon isotopic compositions of algal lipids: Implications for deciphering the carbon isotopic biomarker record. *Geochimica et Cosmochimica Acta* 62: 1397–1406.
- Schulte S, Benthien A, Müller P, and Rühlemann C (2004) Carbon isotopic fractionation (ϵ_p) of C37 alkenones in deep-sea sediments: Its potential as a paleonutrient proxy. *Paleoceanography* 19(1): PA1011.
- Schulz KG, Rost B, Burkhardt S, Riebesell U, Thoms S, and Wolf-Gladrow DA (2007) The effect of iron availability on the regulation of inorganic carbon acquisition in the coccolithophore *Emiliania huxleyi* and the significance of cellular compartmentation for stable carbon isotope fractionation. *Geochimica et Cosmochimica Acta* 71: 5301–5312.
- Scott KM, Henn-Sax M, Longo D, and Cavanaugh CM (2007) Kinetic isotope effect and biochemical characterization of form IA RubisCO from the marine cyanobacterium *Prochlorococcus marinus* MIT9313. *Limnology and Oceanography* 52: 2199–2204.
- Scott KM, Schwedock J, Schrag DP, and Cavanaugh CM (2004) Influence of form IA RubisCO and environmental dissolved inorganic carbon on the $\delta^{13}C$ of the clam-bacterial chemoautotrophic symbiosis *Solemya velum*. *Environmental Microbiology* 6: 1210–1219.
- Seki O, Foster GL, Schmidt DN, Mackensen A, Kawamura K, and Pancost RD (2010) Alkenone and boron-based Pliocene pCO_2 records. *Earth and Planetary Science Letters* 292: 201–211.
- Sekino K, Kobayashi H, and Shiraiwa Y (1996) Role of coccoliths in the utilization of inorganic carbon by a marine unicellular coccolithophorid, *Emiliania huxleyi*: A survey using intact cells and protoplasts. *Plant and Cell Physiology* 37: 123–127.
- Sekino K and Shiraiwa Y (1994) Accumulation and utilization of dissolved inorganic carbon by a marine unicellular coccolithophorid, *Emiliania huxleyi*. *Plant and Cell Physiology* 35: 353–361.
- Sharkey TD and Berry JA (1985) Carbon isotope fractionation in algae as influenced by inducible CO_2 concentrating mechanism. In: Lucas W and Berry JA (eds.) *Inorganic Carbon Uptake by Aquatic Photosynthetic Organisms*, pp. 389–401. Rockville, MD: American Society of Plant Biologists.
- Sikes CS and Wheeler AP (1982) Carbonic anhydrase and carbon fixation in coccolithophorids. *Journal of Physiology* 18: 123–126.
- Stoll MS and Schrag DP (2000) Coccolith Sr/Ca as a new indicator of coccolithophorid calcification and growth rate. *Geochemistry, Geophysics, Geosystems* 1(5): 1006–1024.
- Tabita FR, Satagopan S, Hanson TE, Kreef NE, and Scott SS (2008) Distinct form I, II, III, and IV RubisCO proteins from the three kingdoms of life provide clues about RubisCO evolution and structure/function relationships. *Journal of Experimental Botany* 59: 1515–1524.
- Tcherkez GGB, Farquhar GD, and Andrews TJ (2006) Despite slow catalysis and confused substrate specificity, all ribulose biphosphate carboxylases may be nearly perfectly optimized. *Proceedings of the National Academy of Sciences of the United States of America* 103: 7246–7251.
- Thierstein HR, Geitzenauer KR, Molino B, and Shackleton NJ (1977) Global synchronicity of late Quaternary coccolith datum levels: Validation by oxygen isotopes. *Geology* 5: 400–404.
- Tortell P (2000) Evolutionary and ecological perspectives on carbon acquisition in phytoplankton. *Limnology and Oceanography* 45(3): 744–750.
- Tsuji Y, Suzuki I, and Shiraiwa Y (2009) Photosynthetic carbon assimilation in the coccolithophorid *Emiliania huxleyi* (Haptophyta): Evidence for the predominant operation of the C3 cycle and the contribution of β -carboxylases to the active anaplerotic reaction. *Plant and Cell Physiology* 50: 318–329.
- Van Dongen BE, Schouten S, and Sinninghe Damsté JS (2002) Carbon isotope variability in monosaccharides and lipids of aquatic algae and terrestrial plants. *Marine Ecology Progress Series* 232: 83–92.
- Verity PG, Robertson CY, Tronzo CR, Andrews MG, Nelson JR, and Sieracki ME (1993) Relationships between cell volume and the carbon and nitrogen content of marine photosynthetic nanoplankton. *Limnology and Oceanography* 37: 1434–1446.
- Wolf-Gladrow D and Riebesell U (1997) Diffusion and reactions in the vicinity of plankton: A refined model for inorganic carbon transport. *Marine Chemistry* 59: 17–34.

- Wong WW and Sackett WM (1978) Fractionation of stable carbon isotopes by marine phytoplankton. *Geochimica et Cosmochimica Acta* 42: 1809–1815.
- Young J (1990) Size variation of Neogene Reticulofenestra coccoliths from Indian Ocean DSDP cores. *Journal of Micropalaeontology* 9: 71–86.
- Young J (1998) Neogene. In: Bown P (ed.) *Calcareous Nannofossil Biostratigraphy*, pp. 225–265. Cambridge: Chapman and Hall.
- Young JN, Rickaby REM, Kapralov MV, and Filatov DA (2012) Adaptive signals in algal Rubisco reveal a history of ancient atmospheric carbon dioxide. *Philosophical Transactions of the Royal Society B: Biological Sciences* 367: 483–492.
- Zhang YG, Pagani M, Liu Z, Bohaty SM, and DeConto R (in press) A 40-million-year history of atmospheric CO_2 . *Philosophical Transactions of the Royal Society A*.